Available online at www.sciencedirect.com
ScienceDirect
Lithos 92 (2006) 378–398
LITHOS
www.elsevier.com/locate/lithos

Mineral and fluid inclusions in zircon of UHP metamorphic rocks from the CCSD-main drill hole: A record of metamorphism and fluid activity

Zeming Zhang [a,*], Kun Shen [b], Yilin Xiao [c], Jochen Hoefs [c], J.G. Liou [d]

[a] *Institute of Geology, Chinese Academy of Geological Sciences, 26 Baiwanzhuang Road, Beijing, 100037, China*
[b] *Institute of Geological Sciences of Shandong, Jinan, 250013, China*
[c] *Geoscience Center, Göttingen University, Goldschmidtstrasse 1, D-37077 Göttingen, Germany*
[d] *Department of Geological and Environmental Sciences, Stanford University, Stanford, CA 94305, USA*

Received 16 June 2005; accepted 30 March 2006
Available online 5 July 2006

Abstract

The Chinese Continental Scientific Drilling (CCSD) main drill hole (0–3000 m) in Donghai, southern Sulu orogen, consists of eclogite, paragneiss, orthogneiss, schist and garnet peridotite. Detailed investigations of Raman, cathodoluminescence, and microprobe analyses show that zircons from most eclogites, gneisses and schists have oscillatory zoned magmatic cores with low-pressure mineral inclusions of Qtz, Pl, Kf and Ap, and a metamorphic rim with relatively uniform luminescence and eclogite-facies mineral inclusions of Grt, Omp, Phn, Coe and Rt. The chemical compositions of the UHP metamorphic mineral inclusions in zircon are similar to those from the matrix of the host rocks. Similar UHP metamorphic *P–T* conditions of about 770 °C and 32 kbar were estimated from coexisting minerals in zircon and in the matrix. These observations suggest that all investigated lithologies experienced a joint in situ UHP metamorphism during continental deep subduction. In rare cases, magmatic cores of zircon contain coesite and omphacite inclusions and show patchy and irregular luminescence, implying that the cores have been largely altered possibly by fluid–mineral interaction during UHP metamorphism.

Abundant H_2O–CO_2, H_2O- or CO_2-dominated fluid inclusions with low to medium salinities occur isolated or clustered in the magmatic cores of some zircons, coexisting with low-*P* mineral inclusions. These fluid inclusions should have been trapped during magmatic crystallization and thus as primary. Only few H_2O- and/or CO_2-dominated fluid inclusions were found to occur together with UHP mineral inclusions in zircons of metamorphic origin, indicating that UHP metamorphism occurred under relatively dry conditions. The diversity in fluid inclusion populations in UHP rocks from different depths suggests a closed fluid system, without large-scale fluid migration during subduction and exhumation.

Keywords: Zircon; Mineral and fluid inclusions; Fluid evolution; UHP metamorphism; Drill core; Chinese Continental Scientific Drilling

1. Introduction

Zircon is a common accessory mineral in many rocks, and preserves key petrogenetic information, such as protolith characteristics and formation age, due to its extreme stability and resistance over wide temperatures

* Corresponding author. Tel.: +86 10 68999735; fax: +86 10 68994781.
E-mail address: zzm@ccsd.cn (Z. Zhang).

0024-4937/$ - see front matter © 2006 Elsevier B.V. All rights reserved.
doi:10.1016/j.lithos.2006.04.003

and pressures. Sobolev et al. (1994) and Chopin and Sobolev (1995) considered that zircon is the best container for preserving UHP metamorphic minerals. In the Dabie-Sulu UHP metamorphic belt, coesite and other eclogite-facies minerals have been identified as inclusions in zircon from paragneiss, orthogneiss, amphibolite and marble samples from outcrops (Tabata et al., 1998; Ye et al., 2000; Liu et al, 2001a) and from shallow drill holes (Liu et al., 2001b, 2002). This finding suggests that non-mafic rocks together with eclogites were subjected to in situ Triassic UHP metamorphism. The evolution of fluids in Dabie-Sulu UHP rocks has been extensively discussed on outcrop samples (e.g., Xiao et al., 2000, 2001; Franz et al., 2001; Fu et al., 2001; Xiao et al., 2002; Fu et al., 2003; Zheng et al., 2003; Zhang et al., 2005b). These studies have shown that fluids did exist during UHP metamorphism, and that the fluid compositions and densities are highly variable from different areas.

The drill site of the CCSD is located at the southern segment of the Sulu UHP metamorphic belt (N34°25′, E118°40′), about 17 km southwest of Donghai City (Fig. 1). The CCSD project provides an advantageous and rare chance for collecting UHP rock samples continuously from the subsurface with a depth of more than 5000 m. In this paper we present results of a study on the zoning patterns, mineral and fluid inclusions in zircons of various rocks from the main drill-hole of the CCSD. The purpose of this work is to reveal the protolithic characteristics of the UHP rocks, the relation of eclogites to their gneissic country rocks, and the composition and evolution of UHP metamorphic fluids with spatial and temporal aspects. In comparison with the previous works, the present study has the following progress: (1) coesite and other eclogite-facies mineral inclusions have not only been identified in the metamorphic zircon domains from various rocks, but also found in the zircons of magmatic origin; (2) garnet and omphacite in zircon and those in the matrix of host rock have similar chemical compositions; (3) abundant fluid inclusions occur in the magmatic cores of zircon from most UHP rocks; (4) interactions between fluid inclusions and the host zircons have been commonly identified; (5) fluid inclusion populations vary distinctly with space (depth); moreover, its abundance is related to the oxygen isotopic compositions of the host rocks.

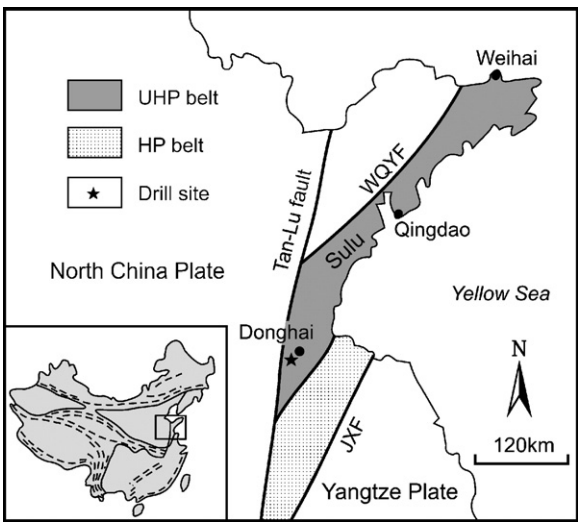

Fig. 1. Simplified geological map of the Sulu UHP metamorphic belt showing major tectonic units and location of the CCSD-main drill hole WQYF = Wulian–Qingdao–Yantai fault, JXF = Jiashan–Xiangshui fault.

Mineral abbreviations used in this paper are after Kretz (1983), except Amp = amphibole, Coe = coesite, Fel = feldspar and Phn = phengite. Other abbreviations are Ec = eclogite, Ogn = orthogneiss, Pgn = paragneiss, Sc = schist, FI = fluid inclusion, and S = solid phase in fluid inclusion.

2. Analytical methods

Zircon was separated by crushing and sieving approximately 250–500 g of each sample, following magnetic and heavy liquid separation. Approximately 100–150 zircon grains from each sample were mounted in epoxy and then polished. Mineral inclusions in zircons were identified using a RENISHAW Raman spectrometer (RM100), at the Key Laboratory for Continental Dynamics of MLR, Institute of Geology, CAGS. Cathodoluminescence of zircon was carried out using a HITACHI S2250-N scanning electron microscope working at 15 kV, ~60 μA, and ~15 mm working distance and a JEOL JXA 8800 electron microprobe at the Physics Department, Peking University, and a JEOL 8900 at the Geoscience center, Göttingen University, respectively. Compositions of exposed mineral inclusions on the polished zircon surface were analyzed using a JEOL JXA 8900 electron microprobe with a 15 kV accelerating voltage and 5 nA beam current, at the Geoscience center, Göttingen University. Microthermometry was performed on fluid inclusions in zircons with a Linkam THM600 freezing–heating stage at the State Key Laboratory for Ore Metallogeny of Nanjing University and the Key Laboratory for Continental Dynamics of MLR. Temperature correction was made by using pure CO_2 inclusions (melting temperature of −56.6 °C), pure water (melting temperature of 0 °C) and potassium dichromate (melting temperature of 398 °C).

For temperatures between −56.6 °C and 0 °C the accuracy is 0.1–0.2 °C; for temperatures between 200 °C and 600 °C, the accuracy is better than 5 °C.

3. Petrology of UHP metamorphic rocks

73 samples, including 42 eclogites and amphibolites, 4 paragneisses, 4 schists, 23 orthogneisses from depths of 0–3000 m of the CCSD-main drill hole were investigated in detail; their locations and major features are shown in Fig. 2 and Table 1. As shown in Fig. 2, the eclogite and orthogneiss, with a total thickness of about 1300 and 1100 m, respectively, are the principal lithologies. Other rock types comprise paragneiss, garnet peridotite and rare schist. Eclogite may contain garnet, omphacite, coesite, phengite, kyanite, zoisite (or epidote), rutile, apatite and zircon as peak-metamorphic minerals. Inclusions of coesite and polycrystalline

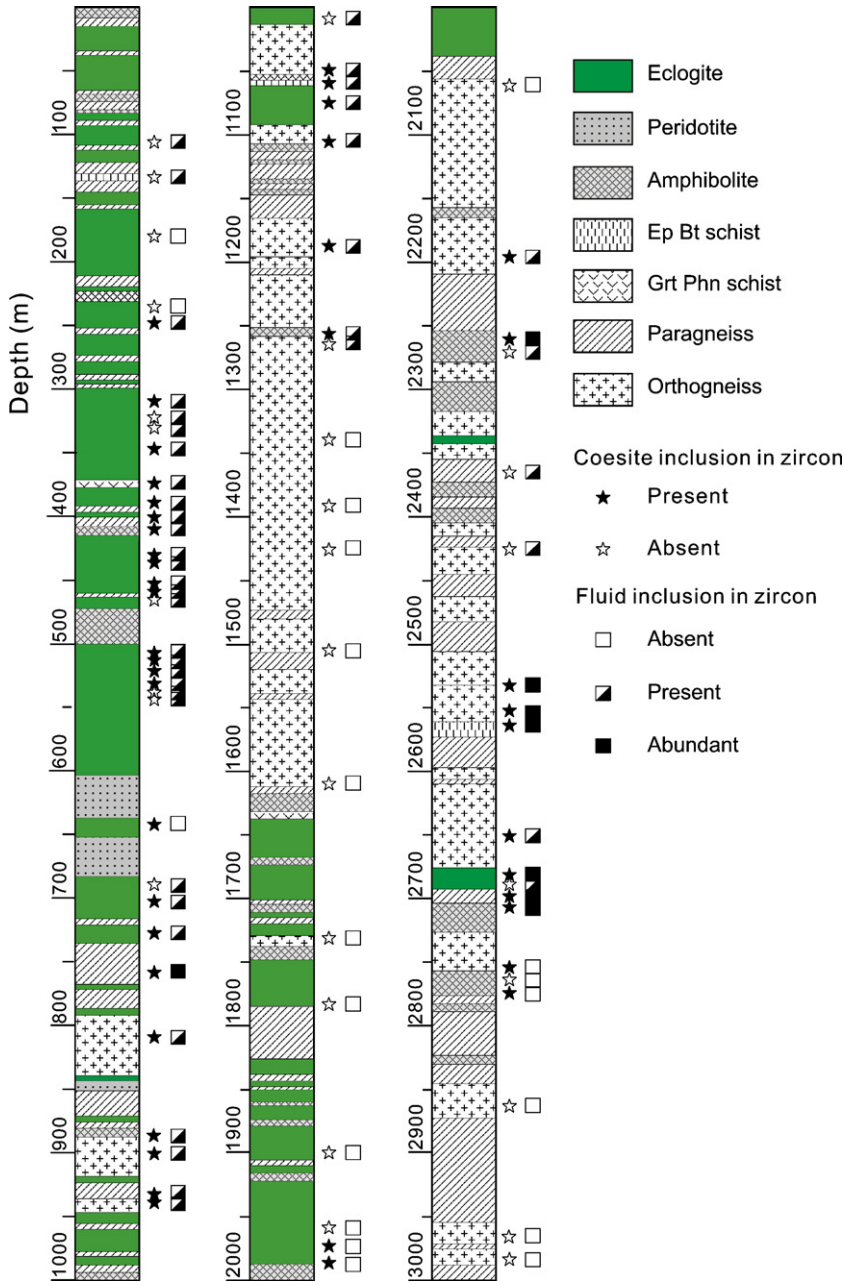

Fig. 2. Lithological profile of the CCSD-main drill hole (0–3000 m), showing the occurrences of coesite and fluid inclusions in zircons.

Table 1
Mineral and fluid inclusions in zircons and matrix mineral assemblages in the host rocks of the representative core samples

Sample	Depth (m)	Rock	Mineral assemblage in matrix	Mineral inclusion in zircon	Fluid inclusion in zircon
ZC62	134.2	Ep Bt schist	Ep, Bt, Pl, Qtz, Ttn	Grt, Omp, Rt, Kf, Ab, Ttn	Present, H_2O
ZA71	174.1	Re.[a] Phn eclogite	Grt, Omp, Phn, Amp, Sym30[b]	Grt, Omp, Phn, Qtz, Rt, Ap, Aug, Pl	Absent
ZA73	249.5	Grt amphibolite	Grt, Amp, Pl, Qtz	Grt, Jd, Phn, Coe, Rt, Ae, Pl, Ab, Kf, Qtz	Abundant, H_2O, CO_2
ZA74	311.7	Re. Phn eclogite	Grt, Omp, Phn, Qtz, Rt, Amp, Sym10	Grt, Omp, Phn, Coe, Amp, Rt, Ap, Qtz	Present, H_2O, CO_2
ZA75	371.3	Grt Phn schist	Grt, Phn, Ep, Bt, Qtz, Rt, Ttn	Grt, Omp, Phn, Coe, Qtz, Ap	Present, H_2O, CO_2
ZA76	387.1	Re. eclogite	Grt, Rt, Amp, Bt, Sym65	Grt, Omp, Phn, Coe, Rt, Ep, Aug, Pl, Qtz, Ap	Present, H_2O, CO_2
ZA77	401.9	Re. eclogite	Grt, Rt, Qtz, Amp, Sym60	Grt, Omp, Phn, Coe, Rt, Qtz, Ap	Abundant, H_2O, CO_2
ZB71	413.6	Re. eclogite	Grt, Omp, Phn, Rt, Qtz, Amp, Sym65	Grt, Omp, Phn, Coe, Rt, Ap, Bt, Pl, Qtz	Abundant, H_2O, CO_2
ZB72	433.0	Rt eclogite	Grt, Omp, Qtz, Rt, Sym5	Grt, Omp, Coe, Rt, Qtz	Present, CO_2
ZC66	452.9	Rt eclogite	Grt, Omp, Ap, Rt, Amp, Qtz	Grt, Omp, Coe, Rt, Ap, Fel, Qtz	Present, H_2O
ZD83	643.8	Re. eclogite	Grt, Bt, Rt, Ttn, Sym45	Grt, Omp, Phn, Coe, Rt, Ap, Amp, Pl, Qtz	Absent
ZG63	687.7	Phn eclogite	Grt, Omp, Phn, Ky, Rt	Grt, Omp, Rt, Ap	Present, H_2O
ZE82	728.0	Eclogite	Grt, Omp, Phn, Rt, Amp, Sym8	Grt, Omp, Phn, Coe, Rt, Ap, Qtz	Present, H_2O
ZE83	812.3	Orthogneiss	Ep, Bt, Pl, Qtz	Grt, Omp, Phn, Coe, Rt, Ap, Fel, Bt, Qtz, Brt	Present, H_2O
ZF71	882.5	Amphibolite	Grt, Amp, Bt, Ep, Pl, Qtz, Rt	Grt, Omp, Phn, Coe, Rt, Ap, Pl, Amp, Qtz, Brt	Abundant, H_2O, CO_2
ZE84	901.9	Orthogneiss	Grt, Ep, Bt, Ms, Pl, Qtz	Grt, Phn, Coe, Rt, Ap, Fel, Qtz	Present, H_2O
ZD85	928.3	Paragneiss	Grt, Zo, Bt, Pl, Qtz, Rt	Grt, Omp, Phn, Coe, Rt, Ap, Fel, Qtz	Present, H_2O, CO_2
ZE85	930.2	Orthogneiss	Grt, Phn, Bt, Pl, Qtz	Grt, Cpx, Phn, Coe, Ap, Fel, Qtz	Present, H_2O
ZD86	1003.4	Eclogite	Grt, Omp, Phn, Qtz, Rt, Zo, Amp, Sym15	Grt, Omp, Phn, Rt, Qtz	Present, H_2O, CO_2
ZF72	1050.3	Orthogneiss	Grt, Ms, Bt, Mt, Pl, Qtz	Phn, Coe, Ap, Brt, Ad, Qtz	Present, H_2O, CO_2
ZE86	1062.2	Ep Bt schist	Ep, Bt, Ttn, Pl, Qtz	Grt, Omp, Phn, Coe, Fel, Br, Ttn, Qtz, Anh	Present, H_2O, CO_2
ZG64	1074.3	Phn eclogite	Grt, Omp, Phn, Sym8	Grt, Omp, Phn, Coe, Rt, Ap, Fel, Qtz	Present, H_2O, CO_2
ZE87	1109.3	Orthogneiss	Grt, Phn, Bt, Pl, Qtz	Grt, Phn, Coe, Ap, Pl, Tnt, Qtz	Present, H_2O, CO_2
ZF73	1183.4	Orthogneiss	Ms, Bt, Pl, Kf, Qtz	Phn, Ap, Ab, Brt, Qtz	Present, H_2O, CO_2
ZG65	1257.9	Amphibolite	Ep, Amp, Bt, Pl, Qtz	Grt, Omp, Phn, Coe, Rt, Ap, Ep, Fel, Brt, Amp, Qtz	Present, H_2O, CO_2
ZF74	1262.1	Orthogneiss	Ms, Pl, Kf, Qtz, Ep	Kf, Qtz, Ap	Absent
ZH63	1263.1	Orthogneiss	Bt, Ms, Pl, Kf, Qtz	Ms, Ab, Kf, Qtz, Cc, Ap, Ttn	Absent
ZH62	1336.9	Orthogneiss	Pl, Kf, Bt, Qtz	Bt, Ab, Kf, Qtz, Ap, Zo	Absent
ZH64	1425.4	Orthogneiss	Zo, Bt, Kf, Pl, Qtz	Kf, Bt, Amp, Qtz, Ap	Absent
ZJ62	2196.8	Orthogneiss	Grt, Amp, Kf, Pl, Qtz, Ep	Phn, Coe, Kf, Ap, Qtz, Ttn	Present, H_2O
ZK64	2362.5	Paragneiss	Ep, Bt, Pl, Kf, Qtz	Omp, Phn, Ab, Ap, Qtz	Present, H_2O
ZJ63	2532.4	Orthogneiss	Grt, Bt, Kf, Pl, Qtz	Grt, Phn, Coe, Rt, Ap, Fel, Qtz, Brt, Ttn	Abundant, H_2O, CO_2
ZI42	2683.1	Re. eclogite	Grt, Ms, Bt, Sym55	Grt, Omp, Phn, Coe, Pl, Qtz	Abundant, H_2O, CO_2
ZK65	2687.0	Re. eclogite	Ep, Bt, Amp, Pl, Sym40	Grt, Omp, Phn, Rt, Ap, Pl, Aug, Qtz	Present, H_2O, CO_2
ZJ66	2698.9	Orthogneiss	Grt, Ep, Bt, Mt, Pl, Kf, Qtz	Grt, Omp, Phn, Coe, Ap, Fel, Amp, Pg, Qtz	Abundant, H_2O, CO_2

[a] Re. retrograde.
[b] Symplectitic minerals and their volume content.

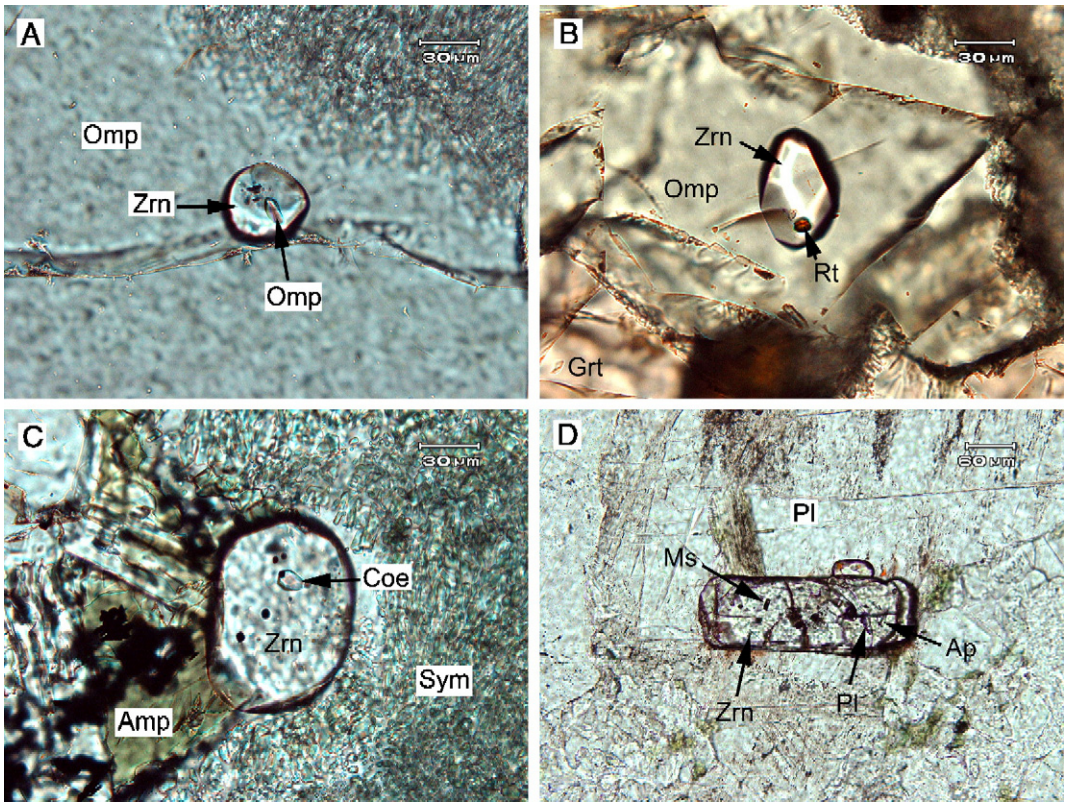

Fig. 3. Microphotography of zircons from eclogite and orthogneiss. (A) Zircon inclusion in eclogitic omphacite (sample ZE82) contains Omp and unknown fine-grained mineral inclusions. The host omphacite was partly replaced by symplectitic corona of Amp+Pl. (B) Zircon inclusion in eclogetic omphacite (sample ZG64) contains Rt inclusion. The host omphacite has thin symplectitic corona of Amp+Pl. (C) Zircon in retrograded eclogite (sample ZA77) contains coesite and unknown fine-grained mineral inclusions. The matrix consists of amphibole, opaque minerals and symplectite (Sym) of Amp+Pl. (D) Zircon inclusion in plagioclase of orthogneiss (sample ZH62) contains Pl, Ms, Ap and unknown fine-grained mineral inclusions.

quartz pseudomorph after coesite are common in garnet and omphacite. Some eclogitic samples have been completely transformed to amphibolite due to amphibolite-facies retrogression. Paragneiss occurs as thin layers, bands or stripes within eclogite and orthogneiss. Schist, including Grt Phn schist and Ep Bt schist, occurs as thin layers or lenses within paragneiss and eclogite. Paragneiss and schist commonly have amphibolite-facies mineral assemblages of Pl, Kf, Qtz, Ep, Bt, with or without Ms, Amp and Grt (Table 1). However, symplectitic pseudomorphs after phengite, omphacite (or jadeite) and garnet were recognized. Coesite and other eclogite-facies mineral inclusions are common in zircons from all paragneisses and schists (see following section).

Orthogneisses can be divided into two types: the first type occurs as intercalated layers with paragneiss and eclogite, showing similar mineral assemblages to paragneiss. This kind of rock also contains rare UHP metamorphic mineral and texture relics. Their zircons have metamorphic overgrowth rim with coesite inclusions. The second type orthogneiss is less foliated and even massive and contains less mafic minerals, occurring at the depth interval from 1200 to 1600 m.

Fig. 4. Plain polarized light (PL, left column) and cathodoluminescence (CL, right column) images of zircons from eclogites. (A) Zircon from sample ZA73 shows an oscillatory zoned magmatic core with Omp inclusions, and a heterogeneous luminescence inner rim with Coe inclusion, and an uncompleted outer rim with bright luminescence. (B) Zircon from sample ZA74 shows an relic magmatic core with broad-band zoning and many fluid inclusions, and a metamorphic domain with Omp and Phn inclusions. (C) Zircon from sample ZD86 shows a thick less intense luminescence core with Grt, Omp and Rt inclusions, and a thin bright-luminescent rim. (D) Zircon from sample ZG64 contains a thick low-luminescence core with Coe and Omp inclusions, and a thin bright-luminescence rim without inclusion. Note that an isolated H_2O+CO_2 fluid inclusion with negative crystal shape occurs in the core of zircon while an Omp inclusion occurs nearby.

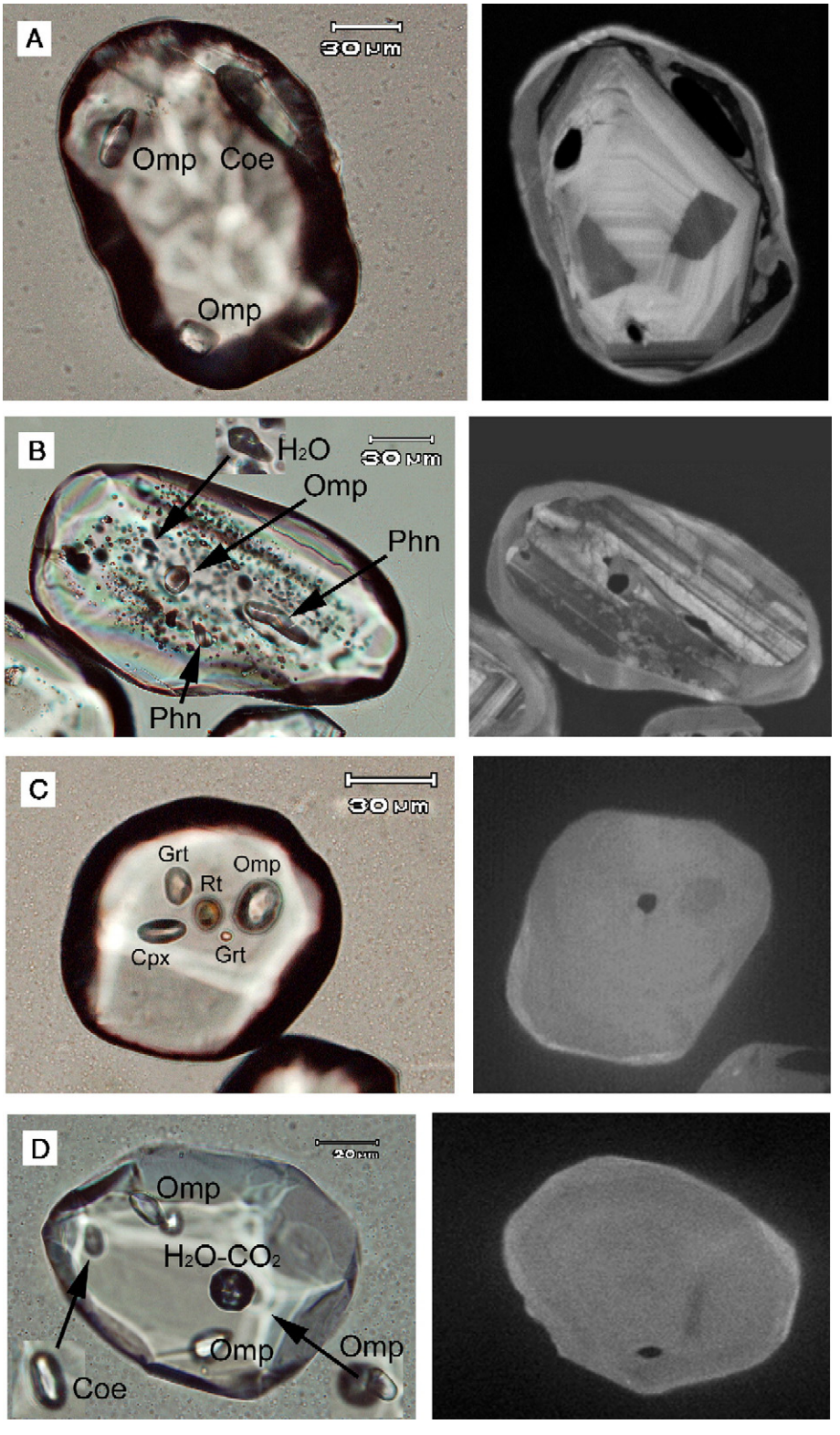
A
30 μm
Omp
Coe
Omp
B
H2O
30 μm
Omp
Phn
Phn
C
30 μm
Grt
Omp
Rt
Cpx
Grt
D
Omp
H2O-CO2
Omp
Omp
Coe

Especially, their zircons are only of magmatic crystallization origin and have no UHP mineral inclusions. The two types of orthogneisses have different geochemical characters, with higher SiO_2, K_2O and Na_2O contents, and distinct negative Eu depletion for the second type (Liu et al., 2004a; Zhang et al., in press).

Zircons in eclogite occur mainly as inclusions in omphacite, garnet, phengite, and symplectitic minerals, and are anhedral to subhedral short-prismatic, rounded and near-spherical, ranging from 50 to 300 μm in length (Figs. 3A–C, and 4). Zircons from paragneiss, schist and orthogneiss of the first type are subhedral short prismatic or near rounded grains, with grain sizes ranging from ca. 50 to 200 μm (Figs. 5A–C and 6). Zircons from the second type orthogneiss are euhedral, prismatic to long prismatic crystal, ranging from 80 to 300 μm in length, and occur mainly as inclusions in Fel, Qtz and Ms (Figs. 3D and 5D).

4. Mineral inclusions in zircon

Based on growth structure and mineral inclusion assemblages of zircons, the investigated zircons were divided into three types: type I has an oscillatory zoned magmatic core with low-*P* mineral inclusions, and one or multilayered metamorphic rims with UHP mineral inclusions. They occur in most eclogites, schists and the first type orthogneiss. Zircons of type II are generally unzoned and contain exclusively UHP mineral inclusions, and occur in some eclogites, paragneiss and schist. Type III occurs only in the second type orthogneiss, and shows euhedral, long prismatic crystals with oscillatory zoning and low-*P* mineral inclusions. They show no metamorphic overgrowth, and are of magmatic origin.

4.1. Mineral inclusions in zircon from eclogite

Based on the Raman analysis, coesite, garnet, omphacite, phengite, rutile, apatite, titanite, diopside, muscovite, plagioclase and quartz were identified as inclusions in zircons from eclogites (Table 1, Figs. 3A–C, 4 and 7A–B). CL images show that zircons from most eclogites have well-developed core and rim structure, i.e., a subhedral to euhedral core surrounded by a subhedral to anhedral rim (Fig. 4A and B), referred as the type I zircon (see above). The cores show concentric oscillatory zoning or broad-band zoning that usually observed for magmatic zircon from mafic intrusives, whereas the rims are unzoned, or show patchy zoning, typical of metamorphic origin (Vavra et al., 1996, 1999; Miller et al., 1998; Schaltegger et al., 1999; Johansson et al., 2001; Rubatto and Scambelluri, 2003). In most zircons, the magmatic cores contain inclusions of Di, Pl, Ms, Qtz and Ap, whereas the metamorphic rims have inclusions of Coe, Grt, Omp, Phn, Rt and Ap. The UHP mineral assemblages included in zircons are generally similar to those in the matrix of the host eclogites (Table 1). In addition, rare barite, anhydrite and magnesite inclusions have been identified. Magnesite is a UHP stable phase in the Dabie-Sulu eclogites (Zhang and Liou, 1994, 1996), but the occurrence of sulfate minerals is not well understood. The UHP mineral inclusions occur not only as isolated phases, but also sometimes in two-mineral associations, i.e. Grt+Omp, Grt+Phn and Omp+Phn. These equilibrium mineral assemblages are used for estimate of *P–T* conditions of the host rocks (see following section).

The magmatic zircon domains commonly show patchy and irregular luminescence (Fig. 4A and B), indicating that they might have been disturbed by a zoning-controlled alteration (Vavra et al., 1999). Moreover, Coe and Omp inclusions are identified in the altered domains. Therefore, we consider that the alteration occurred during UHP metamorphism. Zircon cores with abundant fluid inclusions are more intensively altered (Fig. 4B), indicating that fluids promoted the alteration of zircons, referred to an inclusion-controlled alteration. Zircons from eclogite often have an irregular thin rim with bright luminescence (Fig. 4A, B and C), possibly as a grain boundary alteration (Vavra et al., 1999), or an outermost late growth rim. Zircons from a few eclogitic samples show no zoning and have relatively small grain sizes of 30–150 μm, containing inclusions of Grt, Omp, Coe, Phn and Rt (Fig. 4C and D). They were referred as type II zircons and probably formed during UHP metamorphism.

4.2. Mineral inclusions in zircon from orthogneiss

Zircons from the first type orthogneiss have an oscillatory zoned magmatic core and a metamorphic rim with simple or multilayer zoning (Fig. 5A–C). They are typical of magmatic and metamorphic growth, respectively, as demonstrated by previous works (Vavra et al., 1996, 1999; Miller et al., 1998; Schaltegger et al., 1999; Johansson et al., 2001; Rubatto and Scambelluri, 2003; Rubatto and Hermann, 2003; Sommer et al., 2003). In general, the zircon cores contain Qtz, Fel, Ms, Ep, Ap and Ttn inclusions, whereas the rims contain Grt, Omp, Coe, Phn and Rt inclusions (Table 1). Usually, the oscillatory zoning of zircon cores has been partly

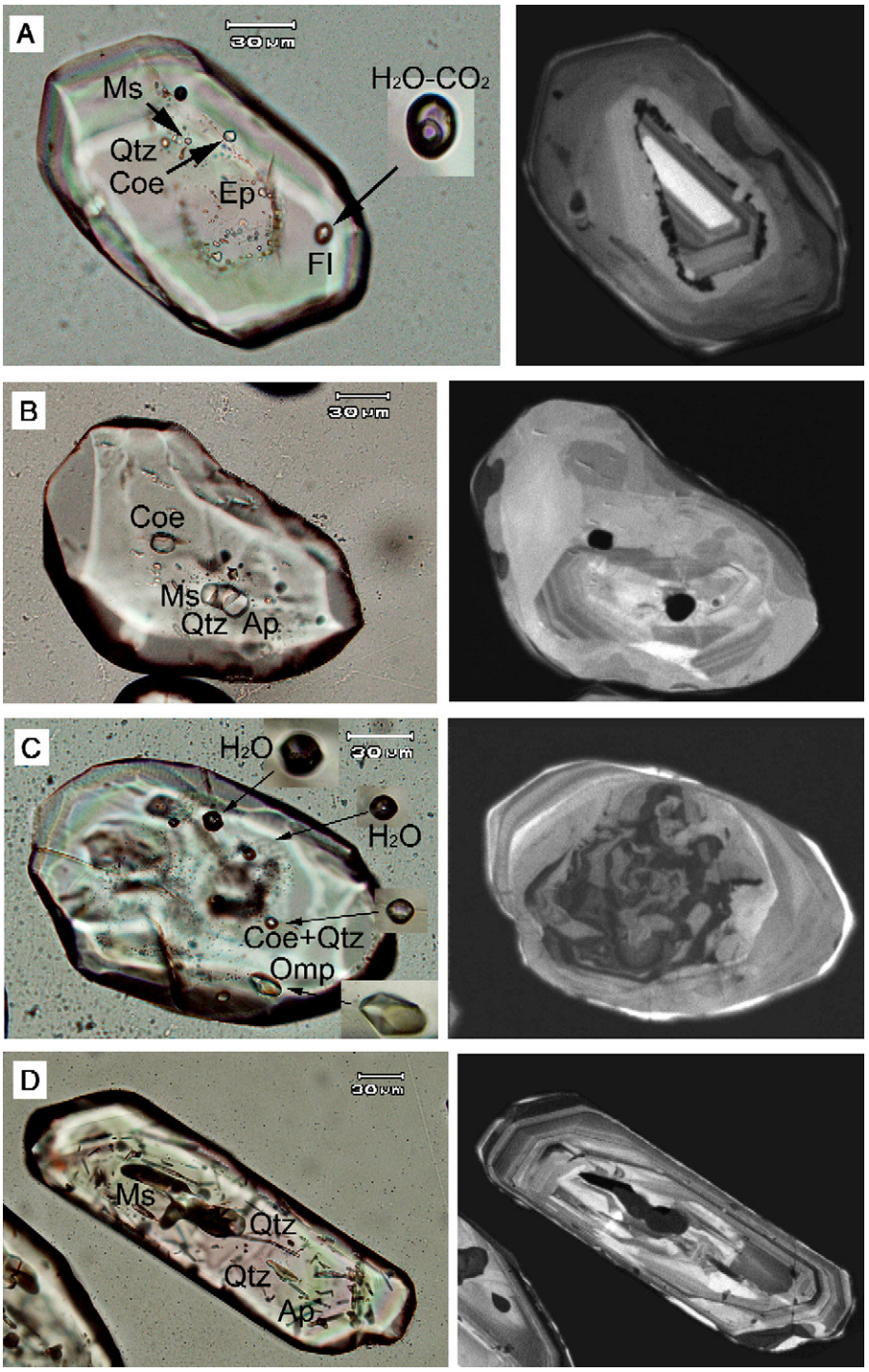

Fig. 5. PL and CL images of zircons from UHP orthogneisses. (A) Zircon from sample ZE87 showing a remnant of an oscillatory zoned magmatic core with inclusions of Ms, Qtz and Ep, and multilayer metamorphic rims with different luminescence, and Coe and H_2O+CO_2 fluid inclusion. (B) Zircon from sample ZF72 showing a magmatic core with oscillatory zoning and inclusions of Ms, Ap and Qtz, and a thick metamorphic rim with patchy luminescence and Coe inclusion. (C) Zircon from sample ZJ66 showing a magmatic core, an inner metamorphic shell and an outer uncompleted shell with bright luminescence. The core shows irregular luminescence, and contains Coe, Qtz and some H_2O fluid inclusions; the metamorphic rim has Omp inclusion. (D) An euhedral, long prismatic zircon from sample ZH64 showing distinct oscillatory zoning, typical of magmatic crystallization, and containing Qtz, Ms and Ap inclusions.

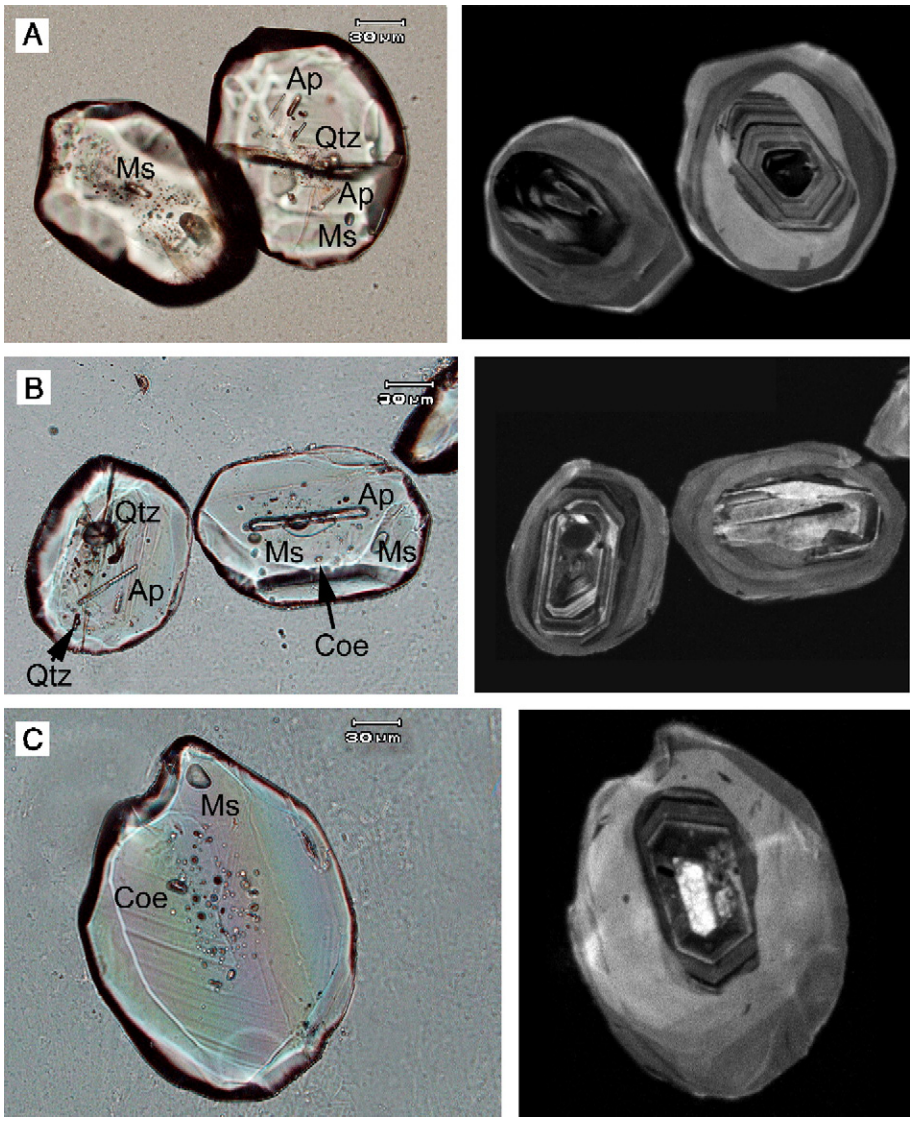

Fig. 6. PL and CL images of zircons from schists. (A) Zircons from sample ZE86 showing an oscillatory zoned magmatic core with Qtz, Ms and Ap inclusions, and three layers of metamorphic rims with different luminescence and inclusion-free. (B) Zircons from sample ZA75 showing an oscillatory zoned magmatic core with Coe, Qtz, Ms and Ap inclusions, and multilayer metamorphic rims with different luminescence. Note that the radial polycrystalline quartz pseudomorph after coesite and the fractures around the inclusion in the left zircon grain. (C) Zircon from sample ZA75 showing an oscillatory zoned magmatic core with Coe and unknown fine-grained mineral inclusions, and metamorphic rims with patchy luminescence and Ms inclusion.

obliterated due to zoning- and/or inclusion-controlled alteration; therefore, the cores show faint zonation or irregular luminescence (Fig. 5B and C).

Zircons from the second type orthogneiss are euhedral, long prismatic crystals, ranging from 80 to 300 μm in length. They usually include only magmatic minerals of Kf, Ab, Qtz, Bt and Ms (Table 1; Fig. 3D and 5D), referred as type III zircon. CL images show that all the zircons have distinct oscillatory zoning, suggesting their magmatic origin.

4.3. Mineral inclusions in zircon from paragneiss and schist

Most zircons from paragneiss are not zoned, and contain Coe, Grt, Omp, Phn and Rt inclusions (Table 1), suggesting their UHP metamorphic origin. Zircons from Grt Phn schist and Ep Bt schist commonly have an oscillatory zoned magmatic core and multilayered metamorphic rims with Coe, Omp, Phn and Grt inclusions (Fig. 6, Table 1). Note that the coesite and

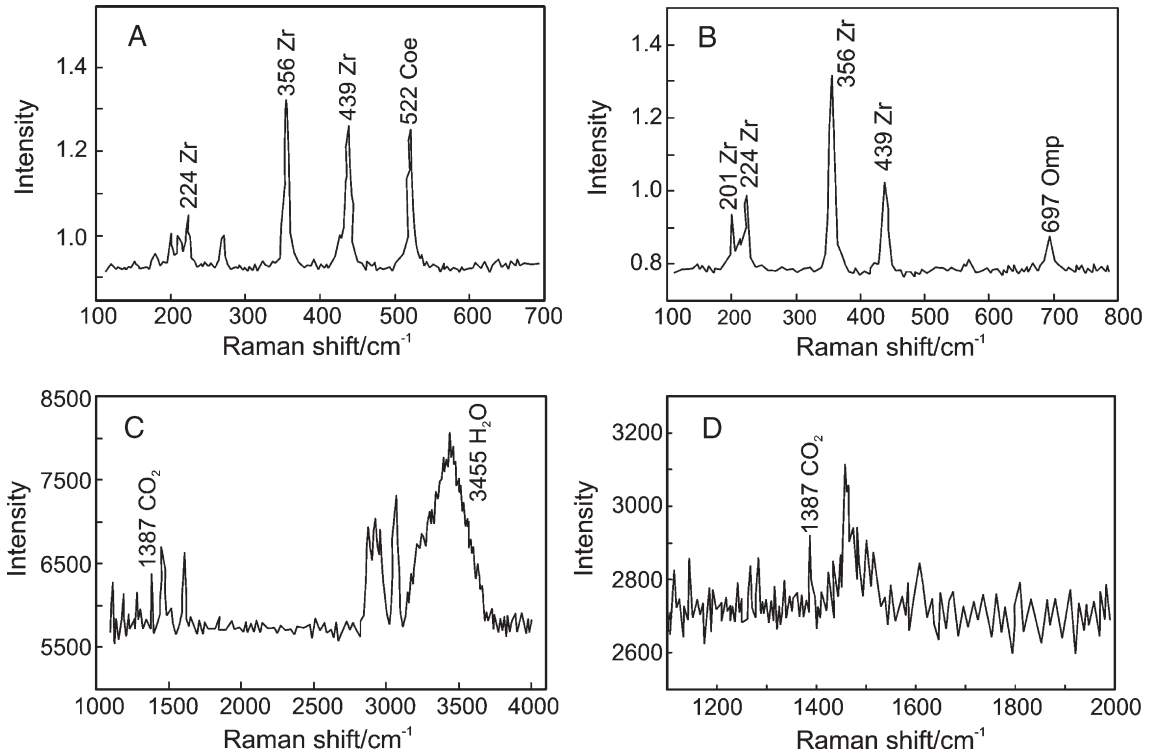

Fig. 7. Raman spectra of mineral and fluid inclusions in zircon from UHP rocks. (A) Coesite inclusion in zircon from eclogite sample (ZA73). (B) Omphacite inclusion in zircon from eclogite sample (ZA73). (C) CO_2–H_2O fluid inclusion in zircon from eclogite sample (ZG64). (D) CO_2 phase of fluid inclusion in zircon from orthogneiss sample (ZF73).

polycrystalline quartz pseudomorph after coesite inclusions are clearly visible within the magmatic core of the zircon (Fig. 6B and C). Like the zircons from other UHP rocks, the oscillatory zoning of zircons from schists has been partly altered, as evidenced by patchy and irregular luminescence (Fig. 6).

5. Compositions of mineral inclusions

Microprobe analyses revealed that mineral inclusions in zircon from various rocks include garnet, omphacite, jadeite, diopside, aegirine, phengite, muscovite, rutile, biotite, plagioclase, albite, K-feldspar, epidote (zoisite), titanite and apatite. Chemical compositions of selected mineral inclusions are listed in Tables 2–6.

5.1. Clinopyroxene

Clinopyroxene inclusions in zircons have a large compositional range. Clinopyroxenes in the metamorphic rims of eclogitic, paragneissic and orthogneissic zircons were identified as omphacite with highly variable jadeite components ranging from 32.1 to 69.2 mol%; a few Cpxs are impure jadeite with 79.4 to 83.4 mol% jadeite components (Fig. 8, Table 2). Clinopyroxenes in the magmatic cores of zircons are diopside, aegirine or aegirine–augite. The Na_2O content of the omphacite inclusions in zircons is similar to that of the matrix omphacites in the host eclogites, with a broad positive correlation between them (Fig. 9). This relation suggests that both of them were formed at the same UHP metamorphic stage.

5.2. Garnet

Almost all garnet inclusions in zircons are of UHP metamorphic origin as they occur in the same zircon domains with omphacite, phengite and coesite inclusions, but they have highly variable compositions. Garnets from the eclogitic zircons range in their major components as $Alm_{26.6–64.0}$, $Prp_{9.0–35.8}$, $Grs_{13.3–37.9}$ and $Sps_{0.5–7.7}$ (Table 3). On the other hand, garnets from zircons of gneisses and schists have very low Prp (2.0–6.0), and relatively high Grs (20.6–42.0) and Sps (3.0–16.0) contents. These garnets are generally similar in composition to those in UHP schists from the Dabie Mountains, but distinctly different from those in the

Table 2
Selected microprobe analyses of clinopyroxene of the investigated rocks

Sample	ZA71-01	ZA71-18	ZA73-15	ZA73-04	ZA73-17	ZA74-9	ZA76-3	ZA76-5	ZA77-5	ZB72-2	ZC66-12	ZD85-4	ZE86-4	ZK65-1	ZK65-4
Rock	Ec	Ec	Ec	Ec	Ec	Ec	Ec	Ec	Ec	Ec	Ec	Pgn	Sc	Ec	Ec
Mineral	Omp	Aug	Jd	Ae	Aug	Omp	Omp	Aug	Omp	Omp	Omp	Aug	Omp	Omp	Aug
SiO_2	57.10	53.02	57.55	54.66	52.62	56.26	56.40	54.47	56.87	55.84	55.43	51.14	53.32	56.78	56.07
TiO_2	0.06	0.16	0.07	0.21	0.13	0.12	0.07	0.03	0.04	0.11	0.14	0.09	0.10	0.09	0.13
Al_2O_3	15.83	3.73	20.03	8.36	1.54	12.99	14.32	4.39	16.61	10.15	8.62	6.35	9.18	14.34	5.79
FeO	2.66	6.69	5.09	16.65	23.81	4.28	4.65	6.98	5.17	7.34	8.68	12.34	10.86	3.28	5.23
MnO	0.02	0.13	0.05	0.41	0.23	0.01	0.00	0.21	0.03	0.02	0.07	0.80	0.64	0.01	0.08
MgO	5.47	12.07	0.66	1.53	2.76	6.55	5.31	11.02	3.25	6.52	7.11	6.89	5.85	6.33	11.06
CaO	9.25	20.63	1.94	3.50	5.86	10.54	8.80	19.50	5.67	10.85	11.71	17.03	12.80	9.87	18.41
Na_2O	9.27	2.76	13.67	12.09	10.41	8.74	9.70	3.24	11.31	8.07	7.28	3.69	6.42	8.61	3.18
K_2O	0.02	0.03	0.03	0.37	0.01	0.01	0.00	0.01	0.03	0.01	0.03	0.00	0.00	0.01	0.00
Total	99.68	99.22	99.09	97.78	97.37	99.50	99.25	99.85	98.98	98.91	99.07	98.33	99.17	99.32	99.95
O	6	6	6	6	6	6	6	6	6	6	6	6	6	6	6
TSi	2.002	1.951	2.000	2.008	2.000	1.987	1.990	1.994	2.001	2.012	2.010	1.942	1.962	2.006	2.042
Ti	0.002	0.004	0.002	0.006	0.004	0.003	0.002	0.001	0.001	0.003	0.004	0.003	0.003	0.002	0.004
Al	0.654	0.161	0.820	0.362	0.069	0.540	0.595	0.189	0.688	0.431	0.368	0.284	0.398	0.597	0.248
Fe^{3+}	0.000	0.126	0.097	0.488	0.691	0.077	0.083	0.052	0.079	0.103	0.116	0.099	0.130	0.000	0.000
Fe^{2+}	0.078	0.080	0.052	0.024	0.066	0.050	0.055	0.162	0.073	0.118	0.147	0.293	0.204	0.096	0.159
Mn	0.001	0.004	0.001	0.013	0.007	0.000	0.000	0.007	0.001	0.001	0.002	0.026	0.020	0.000	0.002
Mg	0.286	0.662	0.034	0.084	0.156	0.345	0.279	0.601	0.170	0.350	0.384	0.390	0.321	0.333	0.601
Ca	0.347	0.813	0.072	0.138	0.239	0.399	0.333	0.765	0.214	0.419	0.455	0.693	0.505	0.374	0.719
Na	0.630	0.197	0.921	0.861	0.767	0.599	0.664	0.230	0.772	0.564	0.512	0.272	0.458	0.590	0.225
K	0.001	0.001	0.001	0.017	0.000	0.000	0.000	0.000	0.001	0.000	0.001	0.000	0.000	0.000	0.000
Cation	3.999	3.999	3.999	3.983	4.000	4.000	4.000	4.000	3.999	4.000	3.999	4.000	4.000	4.000	4.000
Aug	36.1	79.8	8.0	13.0	23.4	39.9	33.4	76.9	22.9	44.0	49.1	72.1	53.4	40.5	76.7
Jd	63.9	9.5	82.3	37.0	7.0	52.5	58.3	18.0	69.2	45.1	38.7	19.4	34.2	59.5	23.3
Ae	0.0	10.7	9.7	50.0	69.7	7.6	8.3	5.1	7.9	10.8	12.2	8.5	12.4	0.0	0.0

Dabie orthogneiss. The latter has higher Sps content, but was speculated to be of UHP metamorphic origin (Carswell et al., 2000).

5.3. Phengite

White mica inclusions in metamorphic rims of eclogitic zircons are identified as phengite with Si values ranging from 3.28 to 3.52 per formula unit (p.f.u.) (O=11) (Table 4). In gneissic zircons, white micas in magmatic cores are muscovite with low Si values of <2.96 p.f.u., whereas those in the metamorphic rims of zircons have high Si value of 3.22–3.43 p.f.u., and are phengite. Rare paragonite inclusions were recognized in magmatic cores of gneissic zircons. All white mica in the metamorphic rims of schistic zircons is phengite with high Si values (3.29–3.56 p.f.u.), being similar to those in the eclogitic zircons.

5.4. Other minerals

Calcic amphiboles, such as tschermakite and tschermakitic hornblende, together with albite and albitic plagioclase, are included in magmatic cores of zircons, representing a relict igneous phase (Table 5). Albite (An<10) and sodic plagioclase (An=13.8 to 28.5) inclusions, together with diopside and amphibole, occur as relict igneous phases in zircon cores from orthogneisses and eclogites (Table 6). Many K-feldspars occur as inclusions in magmatic zircon from orthogneiss. Biotite occurred as relict igneous phase in zircon core of eclogites has low FeO (12.8–19.0 wt.%) and high MgO (10.0–15.0 wt.%) contents; in contrast, biotite included in magmatic zircon without metamorphic rim has relatively high FeO (26.0–28.2 wt.%) and low MgO (4.0–5.1 wt.%) contents. Rutile inclusions in zircons from eclogite and gneiss are pure. Titanite inclusions have variable Fe_2O_3 (up to 3.5 wt.%) and Al_2O_3 (up to 3.6 wt.%) contents. Apatite inclusions contain 53.2–54.6 wt.% CaO, 41.4–42.6 wt.% P_2O_5, and negligible other components.

6. P–T conditions of UHP metamorphism

Peak metamorphic *P–T* conditions of UHP eclogites were usually estimated by equilibrium matrix minerals,

Table 3
Selected microprobe analyses of garnet of the investigated rocks

Sample	ZA74-6	ZA76-11	ZA77-1	ZA77-9	ZB72-5	ZC62-3	ZC66-4	ZD85-02	ZD85-07	ZE84-2	ZG63-7	ZG64-3
Rock	Ec	Ec	Ec	Ec	Ec	Sc	Ec	Pgn	Pgn	Ogn	Ec	Ec
SiO_2	38.67	37.90	37.96	37.66	38.13	37.93	37.84	37.72	37.49	38.04	40.32	39.43
TiO_2	0.06	0.07	0.06	0.02	0.09	0.06	0.06	0.06	0.07	0.02	0.13	0.08
Al_2O_3	21.90	21.28	21.11	20.69	20.99	20.76	21.12	21.13	20.81	21.47	22.51	21.84
FeO	22.91	24.38	25.87	25.91	27.79	22.86	29.21	26.89	24.70	21.88	12.82	18.93
MnO	0.67	1.25	1.40	3.24	0.83	1.42	1.00	1.41	3.78	2.98	0.25	0.41
MgO	5.38	3.94	2.62	2.14	4.88	1.28	5.01	1.55	1.32	1.69	9.49	9.26
CaO	10.16	10.30	10.27	9.20	6.32	14.92	4.94	11.77	11.23	13.81	14.28	9.09
Na_2O	0.01	0.01	0.04	0.05	0.00	0.08	0.02	0.02	0.03	0.02	0.00	0.05
Total	99.76	99.13	99.33	98.91	99.03	99.31	99.20	100.55	99.43	99.91	99.80	99.09
O	12	12	12	12	12	12	12	12	12	12	12	12
TSi	2.999	2.990	3.017	3.025	3.023	3.011	3.002	2.979	3.000	2.998	3.006	3.003
Al	2.000	1.978	1.976	1.957	1.960	1.940	1.973	1.966	1.961	1.992	1.976	1.959
Fe^{3+}	0.074	0.080	0.086	0.087	0.092	0.076	0.097	0.089	0.083	0.072	0.040	0.060
Ti	0.004	0.004	0.004	0.001	0.005	0.004	0.004	0.004	0.004	0.001	0.007	0.005
Fe^{2+}	1.412	1.528	1.633	1.653	1.750	1.442	1.841	1.687	1.570	1.370	0.759	1.146
Mg	0.622	0.463	0.310	0.256	0.577	0.151	0.593	0.183	0.157	0.199	1.055	1.051
Mn	0.044	0.084	0.094	0.220	0.056	0.095	0.067	0.094	0.256	0.199	0.016	0.026
Ca	0.844	0.871	0.874	0.792	0.537	1.269	0.420	0.996	0.963	1.166	1.141	0.742
Na	0.002	0.002	0.006	0.008	0.000	0.012	0.003	0.003	0.005	0.003	0.000	0.007
Cation	8.000	8.000	8.000	8.000	8.000	8.000	8.000	8.000	8.000	8.000	8.000	8.000
Prp	0.21	0.15	0.10	0.09	0.19	0.05	0.20	0.06	0.05	0.07	0.35	0.35
Grs	0.28	0.29	0.29	0.26	0.18	0.42	0.14	0.33	0.32	0.39	0.38	0.25
Alm	0.50	0.53	0.57	0.58	0.61	0.49	0.64	0.57	0.54	0.48	0.27	0.39
Sps	0.01	0.03	0.03	0.07	0.02	0.03	0.02	0.03	0.09	0.07	0.01	0.01

Table 4
Selected microprobe analyses of white mica of the investigated rocks

Sample	ZA71-4	ZA74-7	ZA75-1	ZA76-10	ZA77-3	ZB71-3	ZD85-9	ZE84-1	ZE86-1	ZF73-9	ZH63-1	ZJ66-1	ZK64-7	ZK65-8
Rock	Ec	Ec	Sc	Ec	Ec	Ec	Pgn	Ogn	Sc	Ogn	Ogn	Pgn	Pgn	Ec
SiO_2	50.05	49.61	52.58	51.37	49.45	51.10	45.29	48.34	51.52	49.19	48.44	45.70	48.33	49.17
TiO_2	0.36	0.32	0.50	0.36	0.54	0.55	0.23	0.50	0.49	3.24	0.30	0.04	0.42	0.44
Al_2O_3	26.27	25.26	24.40	23.30	23.97	23.95	27.46	25.12	21.35	21.76	24.55	39.63	25.88	27.80
FeO	1.88	1.92	3.31	2.77	3.00	2.22	6.69	4.48	4.67	6.69	6.03	0.81	4.58	1.84
MnO	0.02	0.01	0.03	0.04	0.04	0.04	0.06	0.07	0.04	0.07	0.11	0.01	0.01	0.01
MgO	3.64	3.88	3.80	4.54	3.65	4.01	1.54	2.72	4.31	2.14	2.75	0.02	2.85	3.20
CaO	0.01	0.05	0.00	0.00	0.03	0.01	0.00	0.00	0.00	0.03	0.00	0.55	0.03	0.00
Na_2O	0.57	0.69	0.08	0.23	0.18	0.23	0.27	0.17	0.03	0.03	0.12	6.31	0.20	0.92
K_2O	10.72	10.03	11.24	10.81	10.88	11.10	10.78	11.09	11.19	11.29	11.16	0.91	11.03	9.79
Total	93.52	91.77	95.94	93.42	91.74	93.21	92.32	92.49	93.60	94.44	93.46	93.98	93.33	93.17
O	11	11	11	11	11	11	11	11	11	11	11	11	11	11
Si	3.409	3.435	3.510	3.516	3.460	3.501	3.223	3.388	3.563	3.428	3.389	2.965	3.356	3.347
Al	2.107	2.059	1.918	1.878	1.975	1.932	2.302	2.073	1.739	1.786	2.023	3.028	2.116	2.228
Ti	0.018	0.017	0.025	0.019	0.028	0.028	0.012	0.026	0.025	0.170	0.016	0.002	0.022	0.023
Fe^{2+}	0.107	0.111	0.185	0.159	0.176	0.127	0.398	0.263	0.270	0.390	0.353	0.044	0.266	0.105
Mn	0.001	0.001	0.002	0.002	0.002	0.002	0.004	0.004	0.002	0.004	0.007	0.001	0.001	0.001
Mg	0.370	0.400	0.378	0.463	0.381	0.410	0.163	0.284	0.444	0.222	0.287	0.002	0.295	0.325
Ca	0.001	0.004	0.000	0.000	0.002	0.001	0.000	0.000	0.000	0.002	0.000	0.038	0.002	0.000
Na	0.075	0.093	0.010	0.031	0.024	0.031	0.037	0.023	0.004	0.004	0.016	0.794	0.027	0.121
K	0.931	0.886	0.957	0.944	0.971	0.970	0.979	0.992	0.987	1.004	0.996	0.075	0.977	0.850
Cation	7.019	7.006	6.985	7.012	7.019	7.002	7.118	7.053	7.034	7.010	7.087	6.949	7.062	7.000

Table 5
Selected microprobe analyses of amphibole of the investigated rocks

Sample	ZA74-4	ZD83-2	ZD86-4	ZF71-02	ZF71-14	ZG65-1	ZG65-4	ZH64-2	ZJ61-3	ZJ66-5
Rock	Ec	Ec	Ec	Ec	Ec	Ec	Ec	Ogn	Ec	Pgn
SiO_2	41.35	40.24	48.24	43.03	42.75	40.87	40.80	38.39	49.43	38.45
TiO_2	0.04	0.65	0.15	0.39	0.71	0.28	0.31	0.22	0.18	0.42
Al_2O_3	9.83	14.59	9.24	11.24	13.61	14.22	15.17	15.39	9.09	13.20
FeO	25.30	17.15	12.53	17.49	19.73	17.46	17.58	25.45	8.18	23.79
MnO	0.51	0.26	0.04	0.40	0.59	0.36	0.37	0.84	0.16	0.80
MgO	5.92	8.55	10.01	9.87	6.50	8.07	7.68	2.61	16.54	5.00
CaO	5.40	11.27	12.52	11.30	10.96	11.33	11.20	10.23	9.07	10.91
Na_2O	6.08	1.87	5.03	1.84	1.80	1.66	1.70	2.68	3.26	1.75
K_2O	0.71	1.73	0.04	0.85	0.57	1.17	1.11	0.47	0.38	1.80
Total	95.14	96.31	97.80	96.41	97.22	95.42	95.92	96.28	96.29	96.12
O	23	23	23	23	23	23	23	23	23	23
Si	6.144	5.981	6.710	6.333	6.334	6.123	6.080	5.833	6.869	5.920
Al	1.720	2.554	1.514	1.948	2.375	2.509	2.662	2.754	1.487	2.394
Ti	0.004	0.073	0.016	0.043	0.079	0.032	0.035	0.025	0.019	0.049
Fe^{3+}	3.144	1.550	1.458	1.664	1.208	1.441	1.389	2.228	0.951	1.838
Fe^{2+}	0.000	0.582	0.000	0.488	1.237	0.747	0.802	1.005	0.000	1.226
Mn	0.064	0.033	0.005	0.050	0.074	0.046	0.047	0.108	0.019	0.104
Mg	1.311	1.894	2.076	2.166	1.436	1.802	1.706	0.591	3.426	1.148
Ca	0.859	1.795	1.866	1.782	1.740	1.819	1.788	1.665	1.351	1.800
Na	1.752	0.539	1.357	0.525	0.517	0.482	0.491	0.790	0.878	0.522
K	0.135	0.328	0.007	0.160	0.108	0.224	0.211	0.091	0.067	0.354
Cation	15.135	15.328	15.007	15.160	15.108	15.224	15.211	15.091	15.067	15.354

Table 6
Selected microprobe analyses of feldspar of the investigated rocks

Sample	ZA71-17	ZA73-16	ZA73-18	ZA73-3	ZA76-6	ZB71-1	ZD83-1	ZH62-3	ZH62-7	ZH63-11	ZH63-2	ZK65-3
Rock	Ec	Ec	Ec	Ec	Ec	Ec	Ec	Ogn	Ogn	Ogn	Ogn	Ec
SiO_2	64.40	64.72	68.15	67.63	64.03	60.52	61.83	64.37	67.35	64.24	68.53	65.83
TiO_2	0.01	0.00	0.05	0.00	0.01	0.00	0.00	0.00	0.00	0.00	0.03	0.00
Al_2O_3	22.12	22.19	20.49	19.59	21.89	24.74	23.72	18.32	19.92	18.24	19.31	20.70
FeO	0.08	0.02	0.02	0.05	0.09	0.07	0.00	0.06	0.02	0.04	0.02	0.06
MnO	0.01	0.00	0.00	0.00	0.00	0.00	0.02	0.00	0.00	0.02	0.03	0.02
MgO	0.06	0.00	0.00	0.00	0.07	0.00	0.00	0.00	0.00	0.00	0.00	0.14
CaO	3.11	2.89	0.74	0.00	3.02	5.89	4.74	0.00	0.80	0.00	0.06	2.01
Na_2O	9.58	9.90	11.43	11.37	10.05	8.10	9.04	0.86	11.08	0.42	11.81	10.64
K_2O	0.16	0.16	0.07	0.70	0.18	0.10	0.29	16.01	0.07	16.45	0.13	0.05
Total	99.53	99.88	100.95	99.34	99.34	99.42	99.64	99.62	99.24	99.41	99.92	99.45
O	8	8	8	8	8	8	8	8	8	8	8	8
Si	11.397	11.411	11.817	11.930	11.380	10.815	11.014	11.960	11.869	11.974	11.991	11.636
Al	4.610	4.608	4.184	4.069	4.582	5.206	4.976	4.009	4.134	4.004	3.979	4.309
Ti	0.001	0.000	0.007	0.000	0.001	0.000	0.000	0.000	0.000	0.000	0.004	0.000
Fe^{2+}	0.012	0.003	0.003	0.007	0.013	0.010	0.000	0.009	0.003	0.006	0.003	0.009
Mn	0.001	0.000	0.000	0.000	0.000	0.000	0.003	0.000	0.000	0.003	0.004	0.003
Mg	0.016	0.000	0.000	0.000	0.019	0.000	0.000	0.000	0.000	0.000	0.000	0.037
Ca	0.590	0.546	0.137	0.000	0.575	1.128	0.905	0.000	0.151	0.000	0.011	0.381
Na	3.287	3.385	3.843	3.889	3.463	2.807	3.122	0.310	3.786	0.152	4.007	3.647
K	0.036	0.036	0.015	0.158	0.041	0.023	0.066	3.795	0.016	3.912	0.029	0.011
Cation	19.950	19.989	20.006	20.053	20.074	19.989	20.086	20.083	19.959	20.051	20.028	20.033
Ab	84.0	85.3	96.2	96.1	84.9	70.9	76.3	7.6	95.8	3.7	99.0	90.3
An	15.1	13.8	3.4	0.0	14.1	28.5	22.1	0.0	3.8	0.0	0.3	9.4
Or	0.9	0.9	0.4	3.9	1.0	0.6	1.6	92.4	0.4	96.3	0.7	0.3

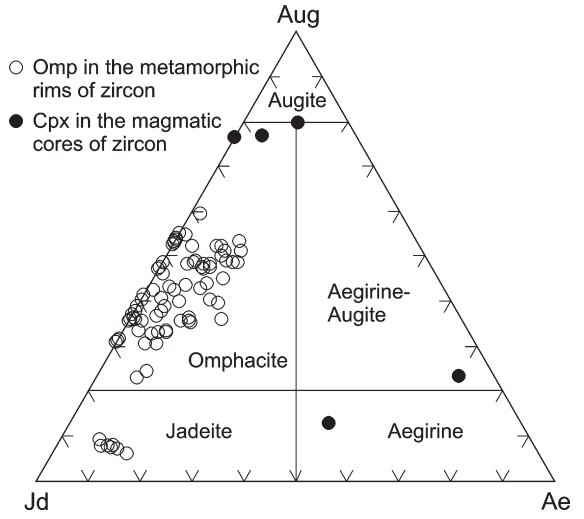

Fig. 8. Compositions of omphacite inclusions in zircons from eclogites.

rather than by isolated mineral inclusions in zircon and other host minerals when they do not in contact with each other and may be in disequilibrium. In this paper, compositions of coexisting two-mineral pairs, such as Grt+Omp and Grt+Phn in metamorphic zircon domains are used as they have the equilibrated contact boundaries and the similar compositions to those from the matrix of host UHP rocks as described above. *P–T* conditions of around 770 °C and 32 kbar were estimated by the Fe^{2+}–Mg distribution geothermometers of garnet–clinopyroxene and garnet–phengite, and the geothermobarometry of phengite–kyanite–coesite eclogite (Green and Hellman, 1982; Ravna, 2000; Ravna and Milke, 2001). These results are similar to those estimated from the matrix mineral assemblages in the host eclogite (Zhang et al., in press), and also to the previous results for the UHP rocks from the outcrops of southern Sulu area (Zhang et al., 1994, 1995; Zhang et al., 1996, 2000). This finding indicates further that the mineral inclusions in the metamorphic zircons were formed at the same metamorphic stage as UHP matrix minerals.

7. Fluid inclusions

Fluid inclusions were found in zircons from most UHP eclogites, orthogneisses and schists. The spatial distribution of fluid inclusion populations is shown in Fig. 2 and listed in Table 1. Based on microthermometry and Raman spectroscopy, three major types of fluid inclusions, namely, H_2O (aqueous)-, CO_2-dominant and mixed H_2O–CO_2 inclusions were distinguished (Fig. 7C–D).

7.1. Fluid inclusions in zircon from eclogites

Isolated or clustered fluid inclusions in eclogitic zircons occur chiefly in the magmatic cores and show rounded or negative crystal shape (Figs. 4B, 10A and B). Tiny fluid and mineral inclusions are concentrated in some zircon cores, forming a cloudy appearance. Fluid inclusion compositions are mainly H_2O, CO_2 and mixed H_2O–CO_2, sometimes with daughter phases such as halite and anhydrite in aqueous inclusions. The core of zircon with fluid inclusions often shows irregular or faint luminescence (Figs. 4B, and 10A–B), implying that the original oscillatory and band zoning has been partly obliterated due to the zoning-controlled and/or the inclusion-controlled alteration. In contrast, minor isolated H_2O–CO_2 inclusions are found in the UHP metamorphic zircon domains where coesite and omphacite inclusions occur (Figs. 4D and 7C). In all probability, they have been trapped during UHP metamorphism.

7.2. Fluid inclusions in zircon from orthogneisses and schists

Abundant fluid inclusions were identified in the magmatic cores of zircons from some orthogneisses, and coexist with Qtz, Ms, Ap and Fel inclusions (Figs. 5C, 10C and D), implying that they were inherited from the magmatic protolith. Such magmatic cores show an irregular luminescence, suggesting that the oscillatory zonation has been partly or completely erased by the inclusion-controlled alteration. Complex H_2O–CO_2 fluid inclusions with solid phases were also found in the core of zircon (Figs. 10D and 7D). Rarely isolated

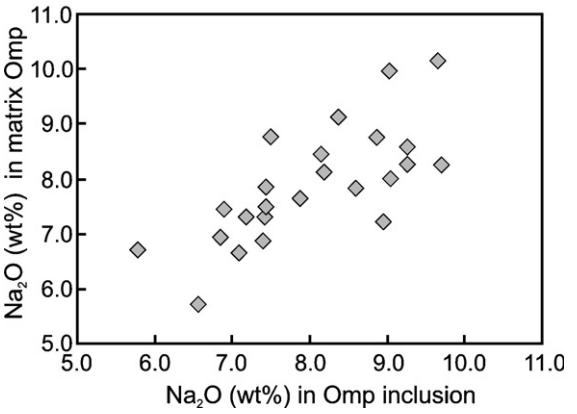

Fig. 9. Correlation of Na_2O content for omphacites in the zircon and matrix of the host eclogites.

H_2O–CO_2 inclusions occur in the coesite-bearing metamorphic rim of zircons from the orthogneiss (Fig. 5A).

7.3. Microthermometry of fluid inclusion

Due to the extremely small size of the investigated fluid inclusions and the highly refractive index of zircon, only a small number of microthermometric measurements could be carried out for the fluid inclusions in the magmatic core of zircons; these data were combined with petrographic observation and Raman analysis to estimate the volume (density)-composition properties of the inclusions. In general, the gas bubble of H_2O inclusions accounts for 10–30% of the total inclusion volume; and the volume percentage of CO_2 phase for mixed H_2O–CO_2 inclusions is similar to that of gas bubble in H_2O inclusions. The eutectic melting temperature of most aqueous inclusions is around −21 °C and the last melting temperature of ice ranges from −12 °C to 0 °C which correspond to salinities of 15 wt.% NaCl eq. to nearly pure water. The homogenization temperature of the inclusions ranges from 120 °C to higher than 200 °C. Hence, the densities of the aqueous inclusions were estimated to be from 0.75 g/cm^3 to 0.98 g/cm^3. In general, the homogenization temperature of CO_2 ranges from 24° to 29 °C by phase transition from CO_2 liquid+CO_2 vapour to liquid; Raman analysis revealed that the CO_2 phase contains nearly pure CO_2. Dissolution temperature of clathrate in a few H_2O–CO_2 inclusions was measured in the range of 3.8~4.2 °C, corresponding to salinities of 10.29–10.87 wt.% NaCl eq. for the aqueous phase in the inclusions. With these data, we are able to calculate the densities of CO_2 and aqueous phases: the density of CO_2 phase ranges between 0.5 and 0.6 g/cm^3 (Angus et al., 1976) and the density of the aqueous phase at room temperature is 1.06 g/cm^3 (Potter and Brown, 1977). By estimating the proportion of H_2O/CO_2 in the H_2O–CO_2 inclusions we then can calculate the bulk density and the composition of the H_2O–CO_2 inclusions using the computer program FLUIDS (Bakker, 2003). The mole fraction of CO_2 and the bulk density of the CO_2–H_2O inclusions are in the range of 0.15–0.3 and 0.75–0.98 g/cm^3, respectively. In summary, the compositions of fluid inclusions in zircon domains of magmatic origin are mainly CO_2–H_2O fluids with salinities ranging from near pure water to more than 10 wt.% NaCl eq. and the densities between 0.75 g/cm^3 and 0.98 g/cm^3, suggesting post-trapping modifications such as fluid–mineral interaction.

8. Discussion and conclusion

8.1. Protoliths of the UHP metamorphic rocks

In spite of the extensive investigations on the petrology and petrochemistry of UHP rocks from the Dabie-Sulu orogenic belt, their protoliths are not well constrained so far. This work shows that eclogites from the CCSD-main drill hole are meta-mafic intrusives as evidenced by the fact that the cores of eclogitic coarse-grained zircons show broad-concentric oscillatory or broad-band zoning patterns, which are usually observed in magmatic zircon from gabbro (Rubatto and Scambelluri, 2003). Geochemical study also shows that the protoliths of the rutile-rich eclogites are of typical layered-gabbro intrusive (Zhang et al., in press). In addition, the protoliths of most gneisses and schists are also magmatic rocks as their zircons have an oscillatory zoned core, typical of felsic intrusive rocks (Miller et al., 1998; Söderlund et al., 2002; Liu et al., 2004a,b). Furthermore, the zircons from the second type orthogneiss have euhedral and long prismatic morphologies, with abundant low-*P* mineral inclusions and distinct oscillatory zoning from the inner core to the outermost rim, indicating that their protoliths are of granitic origin.

8.2. In situ UPH metamorphism

Due to the extensive amphibolite-facies retrograde overprint, the country gneisses of the eclogites commonly have low-*P* mineral assemblages. The present study shows that eclogite-facies minerals occur as inclusions in the metamorphic domains of zircons from eclogite, retrograde eclogite (amphibolite), paragneiss, schist and some orthogneisses. Moreover, these mineral inclusions have similar chemical compositions with those in the matrix of host UHP rocks; similar *P*–*T*

Fig. 10. PL and CL images of zircons from eclogite, schist, and orthogneiss, showing the occurrence of fluid inclusions. (A) Zircon from eclogite (sample ZB72) has a faint zoned magmatic core with Cpx inclusion, and a metamorphic rim without inclusion. H_2O-dominated fluid inclusions occur as clustered in the core of zircon. The oscillatory zoning of zircon core has been highly altered by interaction of the fluid inclusion and host zircon. (B) Zircon from eclogite (sample ZI42) shows locally an oscillatory zoned magmatic core with Ms and H_2O-dominated fluid inclusions, and an irregular metamorphic rim with Grt inclusion. (C) Zircon from schist (sample ZA75) shows an irregular luminescence magmatic core with Ms, Coe, and many fluid inclusions. The metamorphic rim of zircon is inclusion-free. (D) Zircon from orthogneiss (sample ZF73) contains Fel, Qtz and Ap, and complex H_2O–CO_2 fluid inclusions with solid phases and shows broad-concentric zoning.

conditions were also estimated by the coexisting minerals both included in zircons and in the matrix of UHP rocks. These observations strongly suggest that the rocks have been subjected to an early UHP metamorphism before the amphibolite-facies overprint. Furthermore, UHP mineral inclusions like coesite were

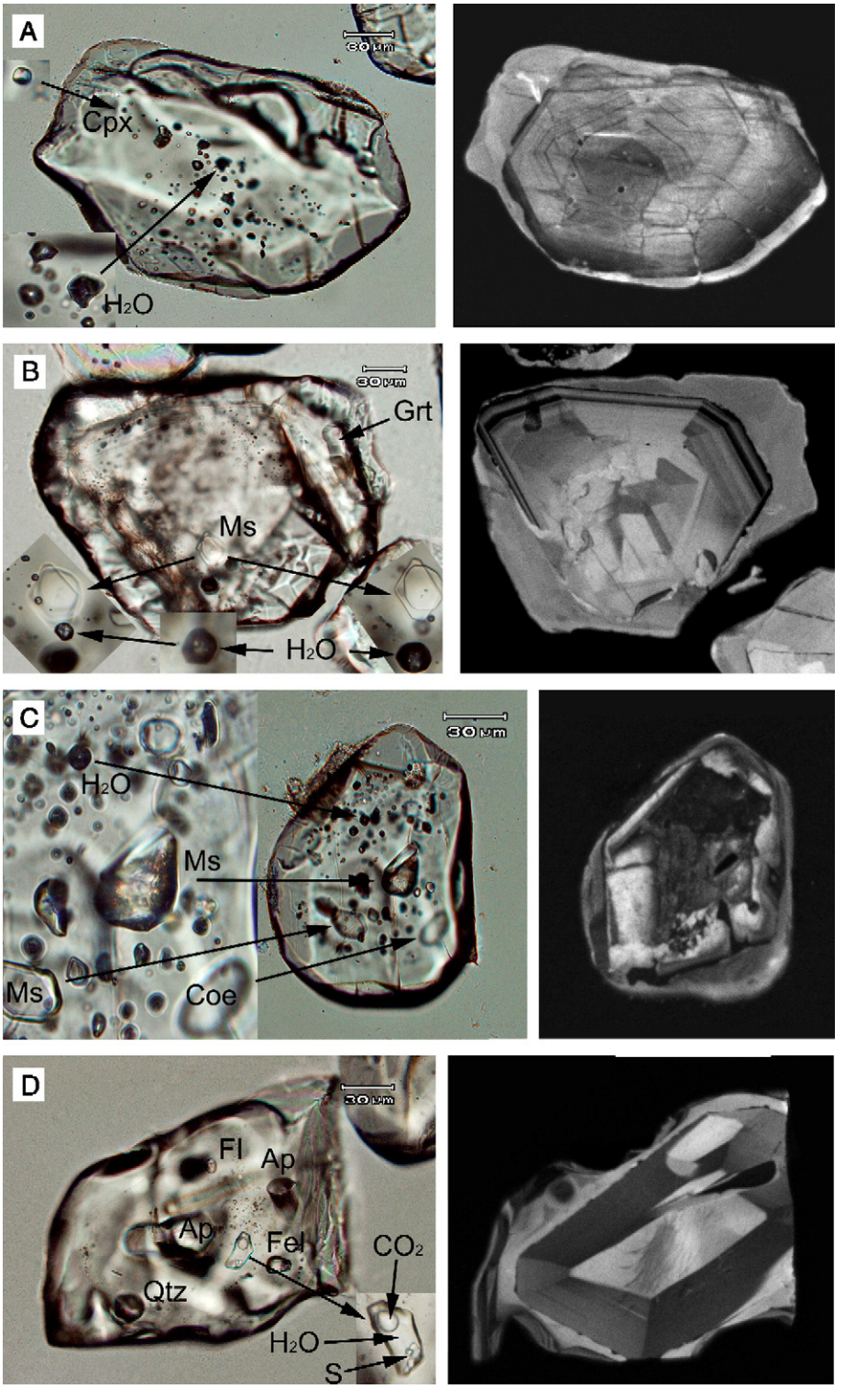

recognized in zircons of various rocks from the depth interval of 3000–5000 m of the CCSD-main drill hole (personal unpublished data). These facts together with the results from some other shallow holes and regional outcrops in Donghai area (Zhang et al., 2000; Liu et al, 2001b, 2002) indicate that voluminous supracrustal materials have been subducted as a coherent continental slab ($>50\times100\times5$ km^3) to mantle depths and returned to the surface.

The zircons of the second type orthogneiss show distinct oscillatory zoning from the core to the rim, and have low-*P* mineral inclusions, typical of zircon crystallized from melt (Vavra et al., 1996, 1999; Miller et al., 1998; Schaltegger et al., 1999; Johansson et al., 2001; Rubatto and Scambelluri, 2003; Sommer et al., 2003). Moreover, UHP mineral relics have not been found in the matrix of the host rocks. These characters suggest that they have not been subjected to the UHP metamorphic event. Similar orthogneisses were already described from the CCSD-PP1 drill hole with a 432-m depth, 17 km NE from the CCSD drill site, and outcrops in the Donghai area (Liu et al., 2001b). Three possible models were proposed for the origin of such orthogneisses. Firstly, they might represent granitic intrusives emplaced after the Triassic UHP event as suggested by Liu et al. (2001b). Secondly, the orthogneisses represent an old granitic intrusive body, which has the same formation age of >680 Ma as the UHP metamorphic orthogneiss (Liu et al., 2004a). However, these protoliths have only been subducted to shallow depths, and emplaced tectonically into UHP metamorphic blocks during exhumation to lower crustal level. Thirdly, the orthogneisses share identical subduction-zone metamorphism at mantle depths; they, however, have not been transformed into UHP metamorphic rocks due to sluggish reaction dynamics. Gebauer et al. (1997) concluded that the resetting of zircons in the orthogneiss from Western Alps even during subduction to mantle depths is apparently a sluggish process, and growth of young metamorphic domains seems to be an exception rather than the rule. In addition, as shown by Oberhänsli et al. (2002), some very low grade metamorphic rocks and basal conglomerates occur as metastable relics in the UHP metamorphic rocks in Dabie. Similarly, relict granulite assemblages in the Western Gneiss region of Norway (Austrheim, 1998) and relict gabbroic and granitic minerals and structures in Yangkou (Hirajima et al., 1993; Zhang and Liou, 1997) in the Sulu UHP terrane have emphasized the role of the fluid for the degree of eclogitization. The present investigation suggests that the orthogneisses without eclogite-facies mineral inclusions show characteristics of lacking fluid inclusions and weak deformation. These features provide strong support for the third possibility.

8.3. Origin of the coesite inclusion in magmatic zircon domains

Available investigations show that zircons are excellent containers for the preservation of UHP minerals (Sobolev et al., 1994; Katayama et al., 2001; Hermann et al., 2001; Liu et al., 2001b, 2002). Although UHP metamorphic rocks have been partly or completely re-equilibrated during decompression, mineral inclusions in zircons are protected from back-reaction and often provide the best evidence for an UHP origin. However, some investigations also demonstrated that the former zircons may have been partly re-crystallized or reset during later thermal events (e.g., Gebauer et al., 1997; Schaltegger et al., 1999; Zeck and Whitehouse, 2002; Tomaschek et al., 2003). The present study shows that inclusions of coesite and polycrystalline quartz pseudomorph after coesite occur in the magmatic domains of zircons from eclogite and schist. In some cases, quartz inclusions together with coesites occur in the UHP growth rim of zircons. Since low-*P* and UHP mineral inclusions may occur together in the UHP metamorphic rim and magmatic core of zircons, interpretation of the association and paragenesis of coesite vs. quartz needs to be done with caution. We argue that zircons are not always the best container for the preventing transformation of mineral inclusions. In addition, it is always not straightforward to derive the relative timing of metamorphic events from mineral inclusions in zircon. Similar coesite and phengite inclusions have been found in magmatic zircon cores of UHP metamorphic rocks from the Dora Maira Massif, Western Alps by Gebauer et al. (1997). They considered that coesite now sealed within magmatic zircon due to successful healing of earlier deformational features is actually a 'pseudo-inclusion' in relation to the whole zircon crystal, and that SiO_2 must have been introduced along cracks of the old zircon to form new coesite in its core. Gillet et al. (1984) speculated that the negative volume change during the transformation of quartz into coesite prevents the coesite growth from a quartz inclusion in the elastic garnet, and the differential elasticity of quartz and garnet cannot alone produce the internal pressure required to stabilize coesite. But we consider that the former quartz inclusions in a fractured grain of magmatic zircon may have transformed to coesite during UHP metamorphism. Although the origin of coesite in magmatic zircon domains has not been well-understood, it is undoubted that some coesite

inclusions in zircon do back-react to polycrystalline quartz (Fig. 6B) as such inclusions of polycrystalline quartz pseudomorphs after coesite are very common in garnet and omphacite of UHP eclogites.

Note that the magmatic cores of zircons, especially those with abundant fluid inclusions, commonly show patchy, irregular or faint luminescence, implying that they have been disturbed by the zoning-controlled alteration and the interaction of the fluid and/or mineral inclusions with host zircon. Moreover, isotopic systems of zircons may have been reset by the alteration. As demonstrated by previous investigations, a large range of and unreasonable ages were obtained by the SHRIMP U–Pb dating on the magmatic core and overgrowth rim of zircons from UHP rocks (e.g., Gebauer et al., 1997; Liu et al., 2004b). Therefore, this study suggests that zircons with complex zoning and abundant fluid and mineral inclusions are not suitable for SHRIMP spot dating. SHRIMP results from such zircons should be explained with caution.

8.4. Fluid composition and evolution during UHP metamorphism

Accessory zircons with growth zoning and associated mineral and fluid inclusions provide a rare chance for understanding the origin and evolution of UHP metamorphic fluids. As mentioned above, zircons from most eclogite and orthogneiss have distinct magmatic cores with oscillatory zoning and low-*P* mineral inclusions. Isolated or clustered fluid inclusions occurred in the magmatic cores of zircons must have been trapped during magma crystallization and may thus represent the fluid composition of the protoliths of these UHP rocks. In contrast, isolated fluid inclusions, which occur only in the zircon rim with metamorphic growth characteristics and coexist with coesite and other eclogite-facies mineral inclusions, might have been trapped during UHP metamorphism and thus represent peak-UHP fluid. In a few eclogites, primary fluid inclusions occur in zircons without any core-rim structure, but with UHP mineral inclusions. They also must have been trapped during peak-UHP metamorphism. Based on Raman analysis, the magmatic and peak-UHP metamorphic fluids trapped in the zircons have similar compositions, i.e., H_2O- and CO_2-dominated, and mixed H_2O–CO_2 fluids. This probably indicates that fluids trapped during UHP metamorphism have been inherited from protolithic fluids. Microthermometric data also demonstrate that primary fluid inclusions in the metamorphic zircons have similar compositions to those of fluid inclusions in UHP matrix minerals of eclogitic rocks (Shen et al., 2005).

Fluid inclusions trapped in magmatic cores of zircons from eclogites and orthogneiss of the first type are relatively abundant, whereas isolated fluid inclusions in the metamorphic zircons are rare. Therefore, we suggest that the UHP metamorphism took place under low fluid activity and that a large amount of fluids may have been expelled out from the protolith of UHP rocks by dehydration and devolatization reactions during prograde metamorphism. Moreover, the fluids remaining in the rock system were mainly incorporated into the structures of hydroxyl-bearing minerals, such as phengite, zoisite and talc, which are stable phases at the peak stage of UHP metamorphism (e.g., Zhang et al., 1995, 2000, 2002, 2003, 2005a), as well as into nominally anhydrous minerals such as garnet and omphacite which can preserve significant amounts of fluids (e.g., Su et al., 2002). Therefore, only a small portion of the fluids was trapped as fluid inclusions.

The fluid evolution of Dabie-Sulu UHP metamorphic rocks has been extensively discussed (e.g., Xiao et al., 2000, 2001; Franz, et al., 2001; Fu et al., 2001, 2003; Zheng et al., 2003; Xiao et al.,2005: Zhang et al., 2005b). Xiao et al. (2000) reported early Ca-rich brines that may have originated from prograde metamorphism and primary NaCl-rich fluids that may have been trapped during the peak of UHP metamorphism. Fu et al. (2003) classified different generations of fluid inclusions in UHP rocks from various locations in the Dabie-Sulu terrane: pre- to syn-peak metamorphic fluids consisting of N_2, CH_4 and high-salinity brines, and post-peak-metamorphic fluids rich in CO_2 and low-salinity water. Investigations on the CCSD pre-pilot hole (PP1), Shen et al. (2003) and Zhang et al. (2005b) suggest that low-salinity H_2O–CO_2 inclusions trapped in topaz from quartzite may originate from a supracrustal protolith. Primary $CaCl_2$–NaCl-rich brine inclusions trapped in garnet and omphacite of eclogite may represent UHP metamorphic fluids. Combining the earlier data with our results, we suggest that the UHP metamorphic fluids vary in composition in different areas of the Dabie-Sulu orogen, and that they may also vary in different protoliths or host minerals as a result of local mineral–fluid reactions.

Our investigations show that fluid inclusions occur mainly in UHP rocks from the depth intervals of 100 to 1250 m, and 2150 to 2720 m; whereas their abundance in the other depth intervals are low (Fig. 2 and Table 1). Moreover, UHP metamorphic rocks enriched in fluid

inclusions have commonly variable degrees of low-oxygen isotopic values. For example, UHP rocks from the depth interval of 2550 to 2700 m, which contain abundant fluid inclusions in zircons, have $\delta^{18}O$ values of −0.35‰ to −7.73‰ and of +2.05 to −2.38‰ for garnet and quartz, respectively; in contrast, UHP rocks from the intervals of 1250 to 2150 m and of 2720 to 3000 m, which have no fluid inclusions in zircons, show $\delta^{18}O$ values of >5.6‰, typical oxygen isotopic compositions for normal metamorphic rocks (Xiao et al., in press). The occurrence of abundant fluid inclusions in UHP metamorphic rocks with unusual low-$\delta^{18}O$ values indicates that their protoliths interacted extensively with meteoric fluids with extremely low oxygen isotope before continental subduction (e.g., Rumble et al., 2002; Zheng et al., 2003, 2005c). In addition, the diversity in fluid inclusion populations and oxygen isotope compositions in UHP rocks from different depths also suggests a closed fluid system without large-scale fluid infiltration during subduction and exhumation of the continental crust.

Acknowledgements

This work has been funded by a Sino-German and Sino-American project related to the Chinese Continental Scientific Drilling. These projects were supported by the Major State Basic Research Development Program (2003CB716501), the National Natural Scientific Foundation of China (40399142, 40472036), the National Science Foundation of Germany (DFG, Ho 375/22), and the US National Science Foundation (EAR 0003355, 0506901). We sincerely thank Profs. Xu Zhiqin, Yang Jingsui, Liu Fulai, You Zhendong and Jin Zhenmin, and Yan Ling, Yong He and the scientists from the Geosciences Centre of University Göttingen for their help in the project. The critical and constructive reviews by Prof. Peter Hans Shertl and Dr. Alfons Van den Kerkhof improved the manuscript significantly.

References

Angus, S., Armstrong, B., de Reuch, K.M., Altuning, V.V., Gedetskii, O.G., Chapela, G.A., Rowlinson, J.S., 1976. International thermodynamic tables of the fluid state. Carbon Dioxide, vol. 3. Pergamon Press, New York. 385 pp.

Austrheim, H., 1998. Influence of fluid and deformation on metamorphism of the deep crust and consequences for the geodynamics of collision zones. In: Hacker, B.R., Liou, J.G. (Eds.), When Continents Collide: Geodynamics and Geochemistry of Ultrahigh-Pressure Rocks. Kluwer Academic & Lippincott Raven.

Bakker, R.J., 2003. Package FLUIDS 1. Computer programs for analysis of fluid inclusion data and for modeling bulk fluid properties. Chem. Geol. 194, 3–23.

Carswell, D.A., Wilson, R.N., Zhai, M.G., 2000. Metamorphic evolution, mineral chemistry and thermobarometry of schists and orthogneisses hosting ultra-high pressure eclogites in the Dabieshan of central China. Lithos 52, 121–155.

Chopin, C., Sobolev, N.V., 1995. Principal mineralogic indicators of UHP in crustal rocks. In: Coleman, R.G., Wang, X. (Eds.), Ultrahigh-Pressure Metamorphism. Cambridge Univ. Press, England, pp. 96–133.

Franz, L., Romer, R.L., Klemd, R., Schmid, R., Wanger, T., Dong, S.W., 2001. Eclogite-facies quartz veins within metabasites of the Dabie Shan (eastern China): pressure–temperature–time–deformation path, composition of the fluid phase and fluid flow during exhumation of high-pressure rocks. Contrib. Mineral. Petrol. 141, 322–346.

Fu, B., Touret, J.L.R., Zheng, Y.F., 2001. Fluid inclusions in coesite-bearing eclogites and jadeite quartzite at Shuanghe, Dabie Shan (China). J. Metamorph. Geol. 19, 529–545.

Fu, B., Touret, J.L.R., Zheng, Y.F., 2003. Remnants of premetamorphic fluid and oxygen isotopic signatures in eclogites and garnet clinopyroxenite from the Dabie-Sulu terranes, eastern China. J. Metamorph. Geol. 21, 561–578.

Gebauer, D., Schertl, H.-P., Brix, M., Schreyer, W., 1997. 35 Ma old ultrahigh-pressure metamorphism and evidence for very rapid exhumation in the Dora Maira Massif, Western Alps. Lithos 41, 5–24.

Gillet, Ph., Ingrin, J., Chopin, C., 1984. Coesite in subducted continental crust: *P–T* history deduced from an elastic model. Earth Planet. Sci. Lett. 70, 426–436.

Green, D.H., Hellman, P.L., 1982. Fe–Mg partitioning between coexisting garnet and phengite at high pressures, and comments on a garnet–phengite geothermometer. Lithos 15, 253–266.

Hermann, J., Rubatto, D., Korsakov, A., Shatsky, V.S., 2001. Multiple zircon growth during fast exhumation of diamondiferous, deeply subducted continental crust (Kokchetav Massif, Kazakhstan). Contrib. Mineral. Petrol. 141, 66–82.

Hirajiama, T., Wallis, S.R., Zhai, M., Ye, K., 1993. Eclogited metagranitoid from the Su-lu ultra-high pressure (UHP) province, eastern China. Proc. Jpn. Acad. 69, 249–254.

Johansson, L., Moller, C., Soderlund, U., 2001. Geochronology of eclogite facies metamorphism in the Sveconorwegian Province of SW Sweden. Precambrian Res. 106, 261–275.

Katayama, I., Maruyama, S., Parkinson, C.D., Terada, K., Sano, Y., 2001. Ion micro-probe U–Pb zircon geochronology of peak and retrograde stages of ultrahigh-pressure metamorphic rocks from the Kokchetav massif, northern Kazakhstan. Earth Planet. Sci. Lett. 188, 185–198.

Kretz, R., 1983. Symbols for rock-forming mineral. Am. Mineral. 68, 277–279.

Liu, J.B., Ye, K., Maruyama, S., Cong, B.L., Fan, H.R., 2001a. Mineral inclusions in zircon from gneisses in the ultrahigh-pressure zone of the Dabie Mountains. China J. Geol. 109, 523–535.

Liu, F., Xu, Z., Katayama, I., Yang, J., Maruyama, S., Liou, J.G., 2001b. Mineral inclusions in zircon of para- and orthogneiss from pre-pilot drillhole CCSD-PP1, Chinese Continental Scientific Drilling Project. Lithos 59, 199–215.

Liu, F.L., Xu, Z.Q., Liou, J.G., Katayama, I., Masago, H., Maruyama, S., Yang, J.S., 2002. Ultrahigh-pressure mineral inclusions in zircons from gneissic core samples of the Chinese Continental

Scientific Drilling Site in eastern China. Eur. J. Mineral. 14, 499–512.

Liu, F.L., Xu, Z.Q., Yang, J.S., Zhang, Z.M., Xue, H.M., Li, T.F., 2004a. Geochemical characteristics and UHP metamorphism of granitic gneisses in the main drilling hole of Chinese Continental Scientific Drilling Project and its adjacent area. Acta Petrol. Sin. 20, 9–26.

Liu, F.L., Xu, Z.Q., Liou, J.G., Song, B., 2004b. SHRIMP U–Pb ages of ultrahigh-pressure and retrograde metamorphism of gneisses, south-western Sulu terrane, eastern China. J. Metamorph. Geol. 22, 315–326.

Miller, C.F., Hatcher, R.D., Harrison, T.M., Coath, C.D., Gorisch, E.B., 1998. Crytic crustal events elucidated through zone imaging and ion microprobe studies of zircon, southern Appalachian Blue Ridge, North Carolina–Georgia. Geology 26, 419–422.

Oberhänsli, R., Martinotti, G., Schmid, R., Liu, X., 2002. Preservation of primary volcanic textures in the ultrahigh-pressure terrain of Dabie Shan. Geology 30, 699–702.

Potter II, R.M., Brown, D.L., 1977. The volumetric properties of aqueous sodium chloride solutions from 0° to 500 °C at pressures up to 2000 bars based on a regression of available data in the literature. U.S. Geol. Surv. Bull. 1421-C, 36.

Ravna, E.K., 2000. The garnet–clinopyroxene Fe^{2+}–Mg geothermometer: an updated calibration. J. Metamorph. Geol. 18, 211–219.

Ravna, K., Milke, P.T., 2001. Geothermobarometry of phengite–kyanite–quartz/coesite eclogites. Eleventh Annual V.M. Goldschmidt Conference. Hot Springs, Virginia, p. 3145.

Rubatto, D., Scambelluri, M., 2003. U–Pb dating of magmatic zircon and metamorphic baddeleyite in the Ligurian eclogites (Voltri Massif Western Alps). Contrib. Mineral. Petrol. 146, 341–355.

Rubatto, D., Hermann, J., 2003. Zircon formation during fluid circulation in eclogites (Monviso, Western Alps): Implications for Zr and Hf budget in subduction zones. Geochim. Cosmoch. Acta 67, 2173–2187.

Rumble, D., Giorgis, D., Ireland, T., Zhang, Z.M., Xu, H.F., Yui, T.F., Yang, J.S., Xu, Z.Q., Liou, J.G., 2002. Low 18O zircons, U–Pb dating, and the Qinglongshan oxygen and hydrogen isotope anomaly near Donghai in Jiangsu Province, China. Geochim. Cosmoch. Acta 66, 2299–2306.

Schaltegger, U., Fanning, C.M., Gunther, D., Maurin, J.C., Schulmann, K., Gebauer, D., 1999. Growth, annealing and recrystallization of zircon and preservation of monazite in high-grade metamorphism: conventional and in-situ U–Pb isotope, cathodoluminescence and microchemical evidence. Contrib. Mineral. Petrol. 134, 186–201.

Shen, K., Zhang, Z.M., van den Kerkhof, A.M., Xiao, Y.L., Xu, Z.Q., 2003. Unusual high-density and saline aqueous inclusions in ultrahigh pressure metamorphic rocks from Sulu terrane in eastern China. Chin. Sci. Bull. 48, 2018–2023.

Shen, K., Zhang, Z.M., Sun, X.M., Xu, L., 2005. Composition and evolution of ultrahigh-pressure metamorphic fluids: a fluid inclusion study of the drill cores from the main hole of Chinese Continental Scientific Drilling Program. Acta Petrol. Sin. 21, 489–504.

Sobolev, N.V., Shatsky, V.S., Vavilov, S.V., Goryainov, S.V., 1994. Zircon from ultrahigh pressure metamorphic rocks of folded regions as an unique containers of inclusions fo diamond, coesite and coexisting minerals. Dokl. Akad. Nauk 334, 488–492 (in Russian).

Söderlund, Ulf., Möller, C., Andersson, J., Johansson, L., Whitehouse, M., 2002. Zircon geochronology in polymetamorphic gneisses in the Sveconorwegian orogen, SW Sweden: ion microprobe evidence for 1.46–1.42 and 0.98–0.96 Ga reworking. Precambrian Res. 113, 193–225.

Sommer, H., Kroner, A., Hauzenberger, C., Muhongo, S., Wingate, M. T.D., 2003. Metamorphic petrology and zircon geochronology of high-grade rocks from the central Mozambique Belt of Tanzania: crustal recycling of Archean and Palaeoproterozoic material during the Pan-African orogeny. J. Metamorph. Geol. 21, 915–934.

Su, W., You, Z.D., Cong, B.L., Ye, K., Zhong, Z.Q., 2002. Cluster of water molecules in garnet from ultrahigh-pressure eclogite. Geology 30, 611–614.

Tabata, H., Yamauchi, K., Maruyama, S., Liou, J.G., 1998. Tracing the extent of a UHP metamorphic terrane: mineral-inclusion study of zircons in gneisses from the Dabieshan. In: Hacker, J.G., Liou, J.G. (Eds.), When Continents Collide: Geodynamics and Geochemistry of Ultrahigh-Pressure Rocks. Kluwer Academic Publishing, London, pp. 261–273.

Tomaschek, F., Kennedy, A.K., Villa, I.M., Lagos, M., Ballhaus, C., 2003. Zircons from Syros, Cyclades, Greece–Recrystallization and mobilization of zircon during high-pressure metamorphism. J. Petrol. 44, 1977–2002.

Vavra, G., Gebauer, D., Schmidt, R., Compston, W., 1996. Multiple zircon growth and recrystallization during polyphase Late Carboniferous to Triassic metamorphism in granulites of the Ivrea Zone (southern Alps): an ion microprobe (SHRIMP) study. Contrib. Mineral. Petrol. 122, 337–358.

Vavra, G., Schmid, R., Gebauer, D., 1999. Internal morphology, habit and U–Th–Pb microanalysis of amphibolite-to-granulite facies zircons: geochronology of the Ivrea Zone (Southern Alps). Contrib. Mineral. Petrol. 134, 380–404.

Xiao, Y.L., Hoefs, J., van den Kerkhof, A.M., Fiebig, J., Zheng, Y., 2000. Fluid history of UHP metamorphism in Dabie Shan, China: a fluid inclusion and oxygen isotope study on the coesite-bearing eclogite from Bixiling. Contrib. Mineral. Petrol. 139, 1–16.

Xiao, Y.L., Hoefs, J., van den Kerkhof, A.M., Li, S.G., 2001. Geochemical constraints of the eclogite and granulite facies metamorphism as recognized in the Raobazhai complex from North Dabie Shan, China. J. Metamorph. Geol. 19, 3–19.

Xiao, Y.L., Hoefs, J., van den Kerkhof, A.M., Simon, K., Fiebig, J., Zheng, Y.F., 2002. Fluid evolution during HP and UHP metamorphism in Dabie Shan, China: constraints from mineral chemistry, fluid inclusions and stable isotopes. J. Petrol. 43, 1505–1527.

Xiao, Y.L., Hoefs, J., Kronz, A., 2005. Compositionally zoned Cl-rich amphiboles from North Dabie Shan, China: monitor of high-pressure metamorphic fluid/rock interaction processes. Lithos 81, 279–295.

Xiao, Y.L., Zhang, Z.M., Hoefs, J., van den Kerkhof, A. in press. Ultrahigh-pressure metamorphic rocks from the Chinese Continental Scientific Drilling Project –II. Oxygen isotope and fluid inclusion distributions through vertical sections. Contrib. Mineral. Petrol.

Ye, K., Yao, Y., Katayama, I., Cong, B.L., Wang, Q.C., Maruyama, S., 2000. Large areal extend of ultrahigh-pressure metamorphism in the Sulu ultrahigh-pressure terrane of East China: new implications from coesite and omphacite inclusions in zircon of granitic gneiss. Lithos 52, 157–164.

Zeck, H.P., Whitehouse, M.J., 2002. Repeated age resetting in zircons from Hercynian–Alpine polymetamorphic schists (Betic Rif tectonic belt, S. Spain)—a U–Th–Pb ion microprobe study. Chem. Geol. 182, 275–292.

Zhang, R.Y., Liou, J.G., 1994. Significance of magnesite paragenesis in ultrahigh-P metamorphic rocks. Am. Mineral. 79, 397–400.

Zhang, R.Y., Liou, J.G., 1996. Significance of coesite inclusions in dolomite from eclogite in the southern Dabie Mountains, China. Am. Mineral. 80, 181–186.

Zhang, R.Y., Liou, J.G., 1997. Partial transformation of gabbro to coesite-bearing eclogite from Yangkou, the Sulu Terrane, eastern China. J. Metamorph. Geol. 15, 183–202.

Zhang, R.Y., Liou, J.G., Cong, B., 1994. Petrogenesis of garnet-bearing ultramafic rocks and associated eclogites in the Su-lu ultrahigh-pressure metamorphic terrane. China J. Metamorph. Geol. 12, 169–186.

Zhang, R.Y., Hirajima, T., Banno, S., Cong, B., Liou, J.G., 1995. Petrology of ultrahigh-pressure rocks from the southern Sulu region, eastern China. J. Metamorph. Geol. 13, 659–675.

Zhang, Z.M., You, Z.D., Han, Y.J., Sang, L.K., 1996. Petrology, metamorphic process and genesis of the Dabie-Sulu eclogite belt Eastern-Central China. Acta Geol. Sin. 9, 134–156.

Zhang, Z.M., Xu, Z.Q., Xu, H.F., 2000. Petrology of ultrahigh-pressure eclogite from the ZK703 drillhole in the Donghai, eastern China. Lithos 52, 35–50.

Zhang, R.Y., Liou, J., Shu, J., 2002. Hydroxyl-rich topaz in high-pressure kyanite quartzites, with retrograde woodhouseite, from the Sulu terrane, eastern China. Am. Mineral. 87, 445–543.

Zhang, Z.M., Xu, Z.Q., Xu, H.F., 2003. Petrology of the non-mafic UHP metamorphic rocks from a drillhole in the Southern Sulu orogenic belt, eastern-central China. Acta Geol. Sin. 77, 173–186.

Zhang, Z.M., Xiao, Y.L., Liu, F., Liou, J., Hoefs, J., 2005a. Petrogenesis of UHP metamorphic rocks from Qinglongshan, Southern Sulu, East-Central China. Lithos 81, 189–207.

Zhang, Z.M., Kun, S., Xiao, Y.L., van den Kerkhof, A.M., Hoefs, J., 2005b. Fluid composition and evolution attending UHP metamorphism: study of fluid inclusions from drill cores, southern Sulu belt, eastern China. Int. Geol. Rev. 47, 297–309.

Zhang, Z.M., Rumber, D., Liou, J.G., Xiao, Y.L., Gao, Y.J., 2005c. Oxygen isotope geochemistry of rocks from the Pre-Pilot Hole of the Chinese Continental Scientific Drilling Project (CCSD-PPH1). Am. Mineral. 90, 857–863.

Zhang, Z.M., Xiao, Y.L., Xu, Z.Q., Hoefs, J., Yang, J.S., Liu, F.L., Liou, J.G., in press. UHP metamorphic rocks from the Chinese Continetal Scientific Drilling Project—I. Petrology and Geochemistry of the Main Hole (0–2050m). Contrib. Mineral. Petrol.

Zheng, Y.F., Fu, B., Gong, B., Li, L., 2003. Stable isotope geochemistry of ultrahigh pressure metamorphic rocks from the Dabie-Sulu orogen in China: implications for geodynamics and fluid regime. Earth-Sci. Rev. 62, 105–161.